# ORIGINAL RESEARCH

Loss of RNF43 Function Contributes to Gastric Carcinogenesis by Impairing DNA Damage Response

Victoria Neumeyer,[1] Anna Brutau-Abia,[1] Michael Allgäuer,[1] Nicole Pfarr,[2] Wilko Weichert,[2] Christina Falkeis-Veits,[3] Elisabeth Kremmer,[4] Michael Vieth,[3] Markus Gerhard,[1] and Raquel Mejías-Luque[1]

[1]Institute for Medical Microbiology, Immunology and Hygiene, School of Medicine, Technical University of Munich, Munich, Germany, [2]Institute of Pathology, Technical University of Munich, Munich, Germany, [3]Institute of Pathology, Klinikum Bayreuth, Bayreuth, Germany, [4]Institute for Molecular Immunology, Helmholtz Zentrum Munich, German Research Center for Environmental Health (GmbH), Monoclonal Antibody Core Facility, Munich, Germany
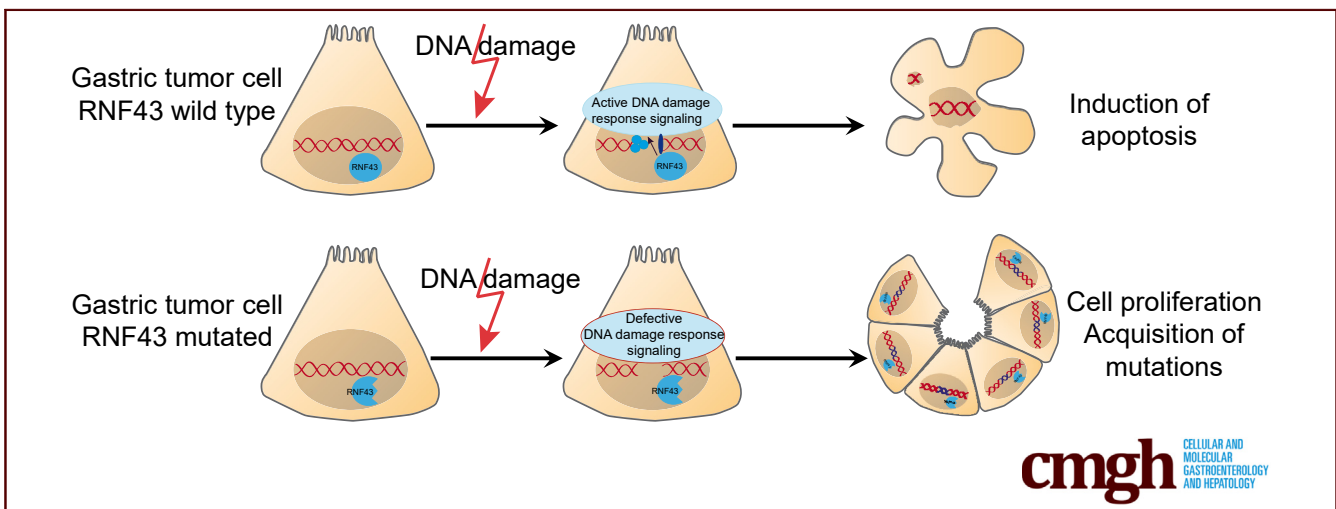
SUMMARY

The tumor-suppressor RING finger protein 43 modulates DNA damage response in gastric cells. The RING finger protein 43 mutational status might be used as a biomarker for therapy selection.

BACKGROUND & AIMS: RING finger protein 43 (RNF43) is a tumor suppressor that frequently is mutated in gastric tumors. The link between RNF43 and modulation of Wingless-related integration site (WNT) signaling has not been shown clearly in the stomach. Because mutations in *RNF43* are highly enriched in microsatellite-unstable gastric tumors, which show defects in DNA damage response (DDR), we investigated whether RNF43 is involved in DDR in the stomach.

METHODS: DDR activation and cell viability upon γ-radiation was analyzed in gastric cells where expression of RNF43 was depleted. Response to chemotherapeutic agents 5-fluorouracil and cisplatin was analyzed in gastric cancer cell lines and xenograft tumors. In addition, involvement of RNF43 in DDR activation was analyzed upon *Helicobacter pylori* infection in wild-type and *Rnf43*$^{\Delta Ex8}$ mice. Furthermore, a cohort of human gastric biopsy specimens was analyzed for RNF43 expression and mutation status as well as for activation of DDR.

RESULTS: RNF43 depletion conferred resistance to γ-radiation and chemotherapy by dampening the activation of DDR, thereby preventing apoptosis in gastric cells. Upon *Helicobacter pylori* infection, RNF43 loss of function reduced activation of DDR and apoptosis. Furthermore, RNF43 expression correlated with DDR activation in human gastric biopsy specimens, and *RNF43* mutations found in gastric tumors conferred resistance to DNA damage. When exploring the molecular mechanisms behind these findings, a direct interaction between RNF43 and phosphorylated H2A histone family member X (γH2AX) was observed.

CONCLUSIONS: We identified a novel function for RNF43 in the stomach as a regulator of DDR. Loss of RNF43 function in gastric cells confers resistance to DNA damage-inducing radiotherapy and chemotherapy, suggesting RNF43 as a possible biomarker for therapy selection. *(Cell Mol Gastroenterol Hepatol 2021;11:1071–1094; https://doi.org/10.1016/j.jcmgh.2020.11.005)*

Gastric cancer (GC) is the fifth most common malignancy and the third leading cause of cancer-related death worldwide (Global Cancer Observatory (GLOBOCAN) 2018). Several attempts have been made to classify gastric tumors to guide treatment selection.[1–3] Despite these numerous attempts, surgery is the only curative treatment available to date. Although the addition of chemotherapy or radiotherapy can improve outcomes, prognosis remains poor, with a median survival of 10–12 months and a 5-year survival rate of <10%.[4] GC patients show a high interindividual as well as intra-individual heterogeneity, making the identification of novel biomarkers indispensable for patient stratification. To date, not many biomarkers for therapy response exist, except for Human epidermal growth factor receptor 2 (HER2) expression or Programmed death-ligand 1 (PD-L1) and microsatellite instability (MSI) levels.[4–6]

Mutations in well-known tumor suppressors, as well as oncogenes such as *TP53* or *KRAS*, have been identified as drivers of GC.[3,7,8] Mutations in the E3 ubiquitin ligase RING finger protein 43 (*RNF43*) also have frequently been reported to occur in microsatellite instability (MSI)-high tumors, suggesting an important role of RNF43 in gastric carcinogenesis.[3,8–12] Recently, we observed that loss of RNF43 function enhances the tumorigenic potential of GC cells in vitro and in vivo,[13] supporting a tumor-suppressor function of RNF43 in the stomach. The tumor-suppressive function of RNF43 has been shown to be related to its capacity to negatively regulate Wingless-related integration site (WNT) signaling by 2 different mechanisms. Located in the cell membrane, RNF43 targets Frizzled receptors for ubiquitin-mediated internalization and degradation, thereby decreasing WNT activity.[14] When expressed in the nucleus, we could show that RNF43 negatively regulates WNT signaling downstream of β-catenin and Adenomatous polyposis coli (APC) by sequestering T-cell factor 4 to the nuclear membrane, thereby suppressing its transcriptional activity.[15] For this inhibitory activity, the presence of an intact RING domain, where the ubiquitin ligase function resides, is essential. Notably, the WNT inhibitory capacity of RNF43 in the stomach has not been completely demonstrated. Our previous results suggested a WNT-independent function of RNF43. Thus, *Rnf43*[ΔEx8] mice carrying an inactivating deletion of the RING domain did not show alterations in the gastric expression of important WNT target genes such as *Axin2* or *Lgr5*. However, we observed thickening of the gastric mucosa, hyperplasia, and cellular atypia in these mice, confirming an important function of RNF43 in gastric homeostasis.[13] Nevertheless, the molecular mechanisms involved remained unknown.

Interestingly, ubiquitination of the main players of the DNA damage response (DDR) is a key event for the activation of this signaling cascade, and several E3 ubiquitin ligases have been reported to be involved.[16–19] The DDR is critical for maintaining genomic stability commonly lost in tumors. Two main kinase-signaling pathways, ataxia-telangiectasia mutated (ATM)–checkpoint kinase 2 (CHK2) and ATM- and Rad3-Related (ATR)–CHK1, coordinate cellular responses to DNA damage. ATM-CHK2 signaling is activated by radiation and genotoxins inducing double-strand breaks (DSBs), while ATR-CHK1 is activated when replication is impeded.[20] Mutations in ATR or CHK1 were found in gastric tumors with MSI,[21] and mutated ATM was associated strongly with MSI,[22] indicating that inhibition of DDR might be important for the development of gastric tumors harboring MSI.

Helicobacter pylori infection, one of the major risk factors for the development of GC, has been linked to DDR. *H pylori* elicits an immune response that leads to the production of reactive oxygen and nitrogen species, which can induce DNA damage.[23,24] In addition, *H pylori* has been shown to induce DSBs directly in host cells.[25,26] Furthermore, *H pylori* infection induces epigenetic modifications leading to the upregulation of ATM.[27] Thus, induction of DNA damage by infection and lack of functional repair mechanisms can highly contribute to gastric carcinogenesis.

Considering the high mutation rate of *RNF43* in gastric tumors showing MSI and our previous data showing that in vivo loss of RNF43 function leads to gastric pathology independent of alterations in WNT signaling,[13] we sought to determine whether RNF43 could be involved in DDR in the stomach and thereby influence response to DNA damage-inducing cancer therapy.

Results
Loss of RNF43 Function Confers Resistance to DNA Damage-Induced Cell Death
To explore whether RNF43 is involved in DDR, we first analyzed the levels of phosphorylated H2A histone family member X (γH2AX) and CHK2 in AGS control and in AGS cells where expression of *RNF43* had been depleted by CRISPR/Cas9 (AGS[deletion at aspartic acid 196 [D196]fs]) (Figure 1*A*). Cellular damage caused by γ-radiation highly induced H2AX and CHK2 phosphorylation in cells expressing RNF43 (Figure 1*B*). Depletion of *RNF43* expression resulted in reduced activation of DDR because lower levels of γH2AX and phosphorylated CHK2 were detected in AGS[D196fs] cells (Figure 1*B*).
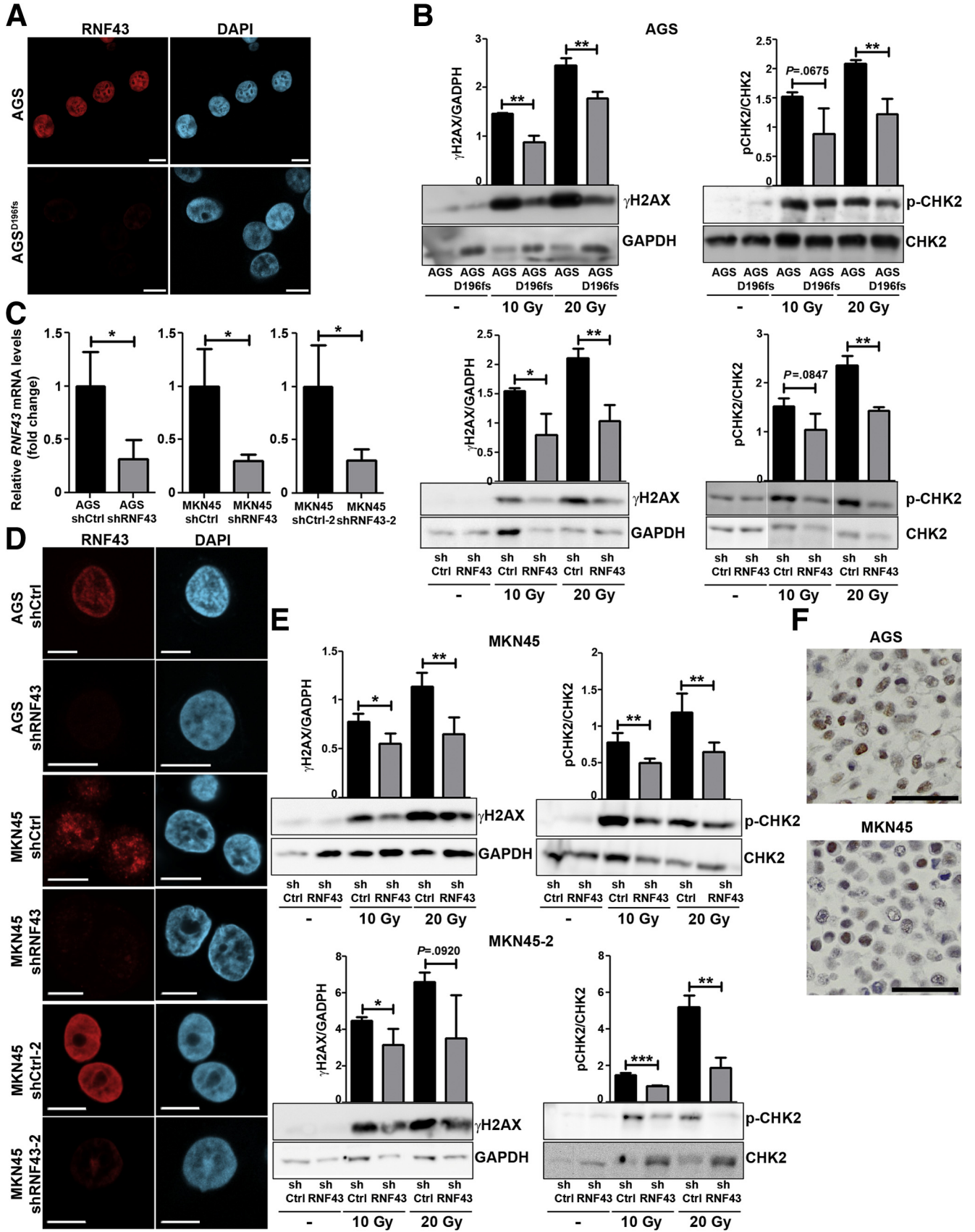
No single clones could be obtained for MKN45 cells after transfection of the guide RNAs. Therefore, we depleted *RNF43* by lentiviral transduction of specific short hairpin RNAs (Figure 1*C* and *D*). Similar to our observations in AGS[D196fs] cells, impaired activation of DDR was observed in MKN45–short hairpin RNF43 (shRNF43) and AGS–shRNF43 cells (Figure 1*E* and *B*, respectively). These observations indicate that RNF43 is important for the induction of DDR in gastric cells.

It has to be noted that AGS and MKN45 cells do not show mutations in *RNF43* (Catalogue Of Somatic Mutations In Cancer (Cosmic) ID: COSS906790 and COSS925340, respectively), and therefore express wild-type (WT) protein in the nucleus (Figure 1*F*).

Interestingly, increased levels of *RNF43* messenger RNA were detected in AGS and MKN45 GC cells after applying different doses of γ-radiation (Figure 2*A*), suggesting that DNA damage induces the expression of RNF43.

We next measured cell viability upon induction of DNA damage through γ-radiation. AGS[D196fs] cells showed enhanced cell viability after irradiation (Figure 2*B*). RNF43 knock-down MKN45 and RNF43 knock-down AGS cells showed increased cell viability compared with short hairpin control (shControl)-transduced cells upon treatment with ionizing radiation (Figure 2*B*). Notably, depletion of *RNF43* either by Clustered related interspaced short palindromic repeats (CRISPR)/ CRISPR associated 9 (Cas9) or short hairpin RNAs already induced changes in cell proliferation under basal conditions (Figure 2*C*), which were accounted for when comparing cell viability of WT and *RNF43*-depleted cells after γ-radiation.

Cell survival after radiation also was assessed in clonogenic assays. Loss of RNF43 enhanced clonal proliferative capacity of gastric cells because more colonies of AGS[D196fs] and MKN45–shRNF43 compared with respective controls were detected after exposing the cells to γ-radiation (Figure 2*D*).

Activation of DDR results in cellular apoptosis when the repair mechanisms cannot cope with the cellular damage inflicted. Thus, we next evaluated whether enhanced viability of cells lacking RNF43 expression upon γ-radiation was the result of reduced cellular apoptosis. We observed that a higher percentage of AGS- and MKN45-expressing WT RNF43 underwent early (Annexin V–positive) and late apoptosis (Annexin V/propidium iodide–double-positive) compared with AGS[D196fs] and MKN45–shRNF43 cells (Figure 2*E*).

Together, our results indicate that RNF43 is involved in DDR in GC cells and depletion of its expression confers resistance to DNA damage-induced apoptosis.

RNF43 Influences Susceptibility to DNA Damage-Inducing Chemotherapeutics

Current GC therapeutic treatments are based on the use of DNA damage-inducing chemotherapeutics, such as cisplatin or 5-fluorouracil.[28] To analyze whether depletion of RNF43 influenced the response of GC cells to DNA damage-inducing chemotherapeutics, we analyzed cell viability in AGS control and AGS[D196fs] cells upon treatment with lethal doses 50 (LD50) of 5-fluorouracil and cisplatin. AGS[D196fs] showed higher cell viability after treatment when compared with control cells (Figure 3*A*), indicating that depletion of RNF43 confers resistance to chemotherapy. Similar results were observed for MKN45–shRNF43 and AGS–shRNF43 cells (Figure 3*A*).

The expression of *RNF43* was increased in AGS and MKN45 cells treated with 5-fluorouracil and cisplatin (Figure 3*B*), confirming up-regulation of RNF43 in response to DNA damage.

Resistance to chemotherapy after depletion of RNF43 expression was explored further in a tumor xenograft model. When tumors originating from MKN45–shControl and MKN45–shRNF43 cells reached 40–70 mm[3], mice were treated with 5-fluorouracil or cisplatin. Tumors derived from MKN45–shRNF43 cells grew bigger compared with tumors that originated from MKN45–shControl cells, as previously reported.[13] Therefore, tumor growth upon treatment with chemotherapeutics was calculated relative to the initial tumor size to account for the growth-promoting effect of RNF43 loss. Tumors derived from MKN45–shRNF43 cells showed enhanced resistance to chemotherapy in vivo because bigger tumors were observed after treatment (Figure 3*C* and *D*), confirming the results observed in vitro. In addition, we evaluated activation of the DDR, apoptosis, and proliferation by staining the tumors for γH2AX, cleaved–caspase 3, and Ki67, respectively, at the end point of treatment with 5-fluorouracil (Figure 4*A*) or cisplatin (Figure 4*B*). Tumors derived from MKN45–shRNF43 cells showed reduced levels of γH2AX upon treatment with 5-fluorouracil, indicating lower activation of DDR (Figure 4*A*). Furthermore, reduced apoptosis and increased proliferation were observed in MKN45–shRNF43–derived tumors (Figure 4*A*) compared with tumors that originated from MKN45–shControl cells. Likewise, after treatment with cisplatin, tumors derived from MKN45–shRNF43 cells showed reduced DDR activation and apoptosis (Figure 4*B*). These tumors also were more proliferative compared with tumors originating from MKN45–shControl cells (Figure 4*B*). Together, these results

---

Figure 1. (*See previous page*). RNF43 is involved in DDR. (*A*) Representative immunofluorescence images of RNF43 (red) in control and AGS[D196fs] cells. *Scale bars*: 10 μm. (*B*) Western blot analysis and quantification of γH2AX and CHK2 expression in WT AGS, AGS[D196fs], control AGS (shCtrl), and RNF43 knockdown AGS (shRNF43) cells after γ-radiation. GAPDH was used as a protein loading control (N = 3). (*C*) *RNF43* mRNA levels in control and RNF43 knockdown AGS and MKN45 cells. Cycle threshold (C_T)values were normalized to *GAPDH* and fold change was calculated over control cells. (*D*) Representative immunofluorescence images of RNF43 (red) in control and RNF43 knockdown AGS and MKN45 cells. *Scale bars*: 10 μm. (*E*) Western blot analysis and quantification of γH2AX and CHK2 expression in control MKN45 (shCtrl) and RNF43 knockdown MKN45 (shRNF43) cells after γ-radiation. GAPDH was used as a protein loading control (N = 3). (*F*) Endogenous RNF43 expression in AGS and MKN45 cells detected by immunocytochemistry. *Scale bar*: 50 μm. Error bars indicate SD. *$P \leq$ .05, **$P \leq$ .01, ***$P \leq$ .001, 2-tailed unpaired *t* test. DAPI, 4′,6-diamidino-2-phenylindole; GAPDH, glyceraldehyde-3-phosphate dehydrogenase; mRNA, messenger RNA.

suggest that, in the absence of RNF43, GC cells become resistant to chemotherapeutics.

To further substantiate resistance to DNA damage-inducing chemotherapeutics after loss of RNF43 function, we generated gastric organoids from WT and $Rnf43^{\Delta Ex8}$ mice.[13] Organoids were treated with 5-fluorouracil or cisplatin, and cell viability was measured after 4 days. Organoids derived from $Rnf43^{\Delta Ex8}$ mice were more resistant
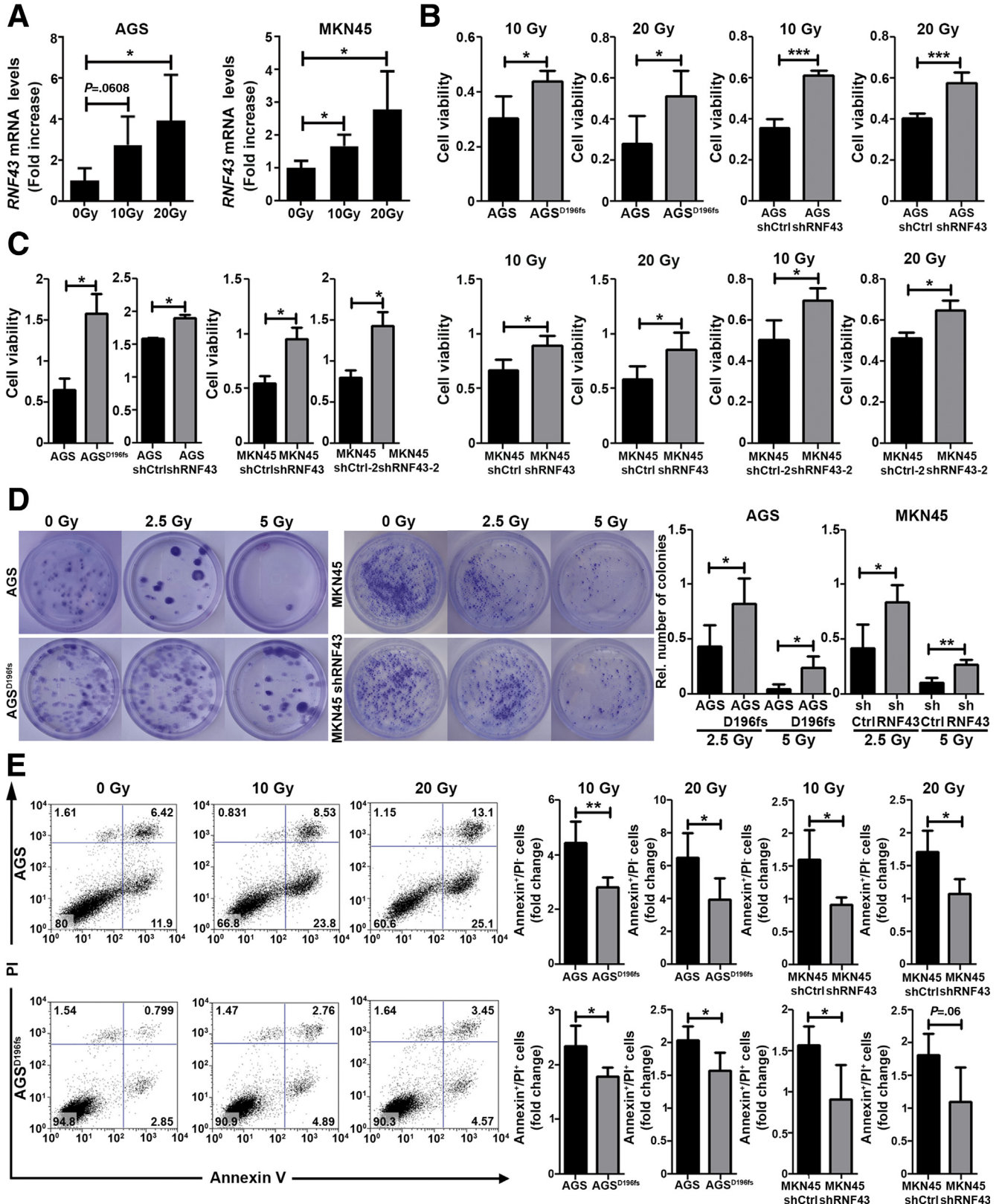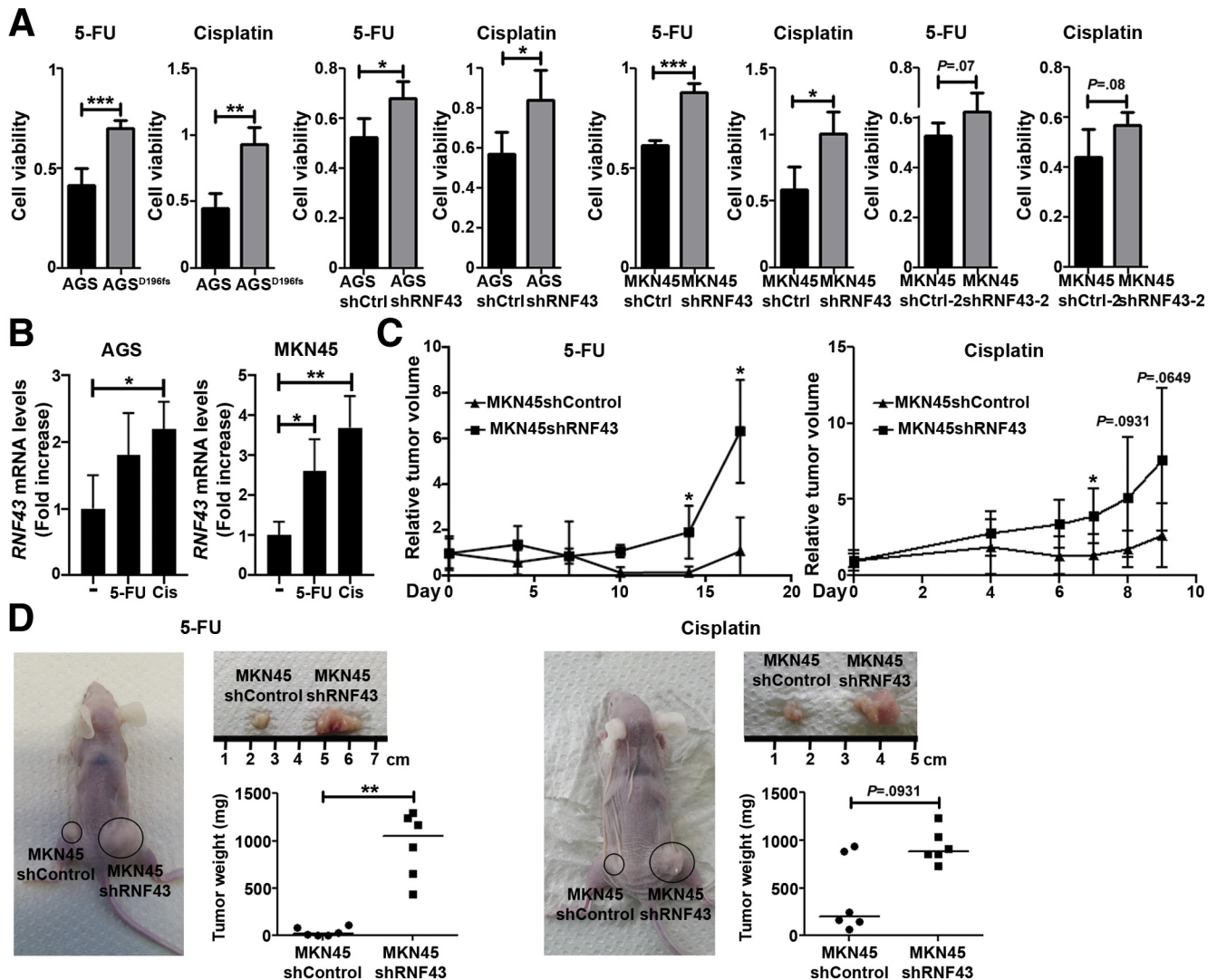
Figure 3. RNF43 influences susceptibility to DNA damage-inducing chemotherapeutics. (*A*) Cell viability of WT AGS, AGS[D196fs], control MKN45 and AGS (shCtrl), and RNF43 knockdown MKN45 and AGS (shRNF43) cells after treatment with 5-fluorouracil (5-FU) or cisplatin. Values were normalized over untreated cells (N = 3). (*B*) *RNF43* mRNA levels in AGS and MKN45 GC cells after treatment with 5-FU or cisplatin (Cis) for 48 hours. Cycle threshold (C_T) values were normalized to *GAPDH* and fold change was calculated over untreated cells (N = 3). (*C*) Relative volume of xenograft tumors derived from control MKN45 (shCtrl) and RNF43 knockdown MKN45 (shRNF43) cells after treatment of mice with 5-FU or cisplatin. Relative volumes were calculated over tumor volume before treatment (N = 6/group). (*D*) Representative images of xenograft tumors derived from control MKN45 (shCtrl) and RNF43 knockdown MKN45 (shRNF43) cells after treatment of mice with 5-FU or cisplatin. Size and weight of the resected tumors are shown (n = 6/group). Error bars indicate SD. *Horizontal lines* represent the median values. *$P \le .05$, **$P \le .01$, and ***$P \le .001$, (*A* and *B*) 2-tailed unpaired *t* test, (*C* and *D*) Mann–Whitney test.

to treatment with chemotherapeutics inflicting DNA damage (Figure 4*C*), confirming the results observed in vitro and in the xenograft model.

Finally, we assessed whether levels of RNF43 correlate with response to chemotherapy using human gastric organoids. Organoids were generated from stomach biopsy specimens

Figure 2. (*See previous page*). **Loss of RNF43 function confers resistance to DNA damage-induced cell death.** (*A*) *RNF43* mRNA levels in AGS and MKN45 gastric cancer cells upon increasing doses of γ-radiation. Cycle threshold (C_T) values were normalized to *GAPDH* and fold change was calculated over untreated cells (N = 4). (*B*) Cell viability of WT AGS, AGS[D196fs], control MKN45 (shCtrl), and RNF43 knockdown MKN45 (shRNF43) cells after γ-radiation. Values were normalized over untreated cells (N = 4). (*C*) Cell viability of AGS, AGS[D196fs] cells, as well as control AGS and MKN45 (shCtrl) and RNF43 knockdown AGS and MKN45 (shRNF43) cells under basal conditions (N = 3). (*D*) Representative images and quantification of cell colonies after γ-radiation (N = 4). (*E*) Flow cytometry analysis of Annexin V and propidium iodide (PI)-positive AGS and MKN45 cells after irradiation. Values were normalized over untreated cells (N = 4). Error bars indicate SD. *$P \le .05$, **$P \le .01$, ***$P \le .001$, 2-tailed unpaired *t* test. mRNA, messenger RNA.

and treated with 5-fluorouracil or cisplatin for 5 days, after which cell viability was measured. An inverse correlation between response to 5-fluorouracil treatment and RNF43 expression was observed (Spearman r_s = -6264; P = .0220) (Figure 4D). RNF43 expression was higher in organoids responding to 5-fluorouracil than in organoids not responding (Figure 4D). Similar results were detected when human gastric organoids were treated with cisplatin (Figure 4E).

These results suggest that cells lacking RNF43 function become resistant to DNA damage-inducing chemotherapeutics.

Because RNF43 has been described to inhibit WNT signaling in different cellular models, we analyzed whether the effects induced by depleting RNF43 expression depended on alterations in WNT. We assessed the expression levels of the WNT target genes $AXIN2$ and $LGR5$ in AGS control and AGS^{D196fs} and MKN45–shControl and MKN45–shRNF43. No differences in the expression of these genes were detected (Figure 4F), indicating that the effects are independent of changes in WNT signaling.

RNF43 Is Involved in H pylori–Induced DNA Damage Response

H $pylori$ has been described to induce DNA damage in gastric epithelial cells.[25] We analyzed whether activation of DDR in response to H $pylori$ infection is compromised in cells with suppressed $RNF43$ expression. Indeed, we observed that activation of DDR, as assessed by H2AX and CHK2 phosphorylation, was reduced in AGS^{D196fs} cells (Figure 5A), indicating that RNF43 is involved in DDR elicited by H $pylori$. Likewise, impairment of DDR in response to H $pylori$ infection was detected in MKN45–shRNF43 and AGS–shRNF43 cells (Figure 5A).

H $pylori$ infection up-regulated the expression of $RNF43$ in AGS and MKN45 cells (Figure 5B). In addition, we observed that the expression of $RNF43$ was higher in gastric biopsy specimens from H $pylori$–infected patients compared with noninfected individuals (Figure 5C).

To further explore the involvement of RNF43 in DDR upon H $pylori$ infection in vivo, we infected WT or $Rnf43^{\Delta Ex8}$ mice with the H $pylori$ pre-mouse SS1 (PMSS1) strain and killed them after 3 months. As previously reported, at this age, $Rnf43^{\Delta Ex8}$ mice did not show pathologic changes in the stomach.[13] H $pylori$ infection up-regulated the expression of $Rnf43$ in the stomach of WT mice (Figure 5D). Notably, $Rnf43^{\Delta Ex8}$ mice were colonized at lower levels than WT mice (Figure 6A) and showed more severe gastric inflammation (Figure 6A). Increased recruitment of CD3$^+$ cells into the stomach was observed in $Rnf43^{\Delta Ex8}$ mice when compared with WT infected mice (Figure 6A). In addition, increased infiltration of neutrophils and mast cells was detected in $Rnf43^{\Delta Ex8}$ mice (Figure 6A). Concomitantly, $Rnf43^{\Delta Ex8}$ mice showed increased expression levels of the proinflammatory cytokines $Cxcl1$ (murine homologue of interleukin 8), $Ifng$, and $Tnfa$ (Figure 6B).

We next assessed activation of DDR response upon H $pylori$ infection by analyzing γH2AX-positive cells in the stomach of WT and $Rnf43^{\Delta Ex8}$ mice. H $pylori$ infection resulted in increased levels of γH2AX-positive cells in WT mice. In contrast, no increase in the induction of DDR was detected in infected $Rnf43^{\Delta Ex8}$ mice, which showed lower numbers of γH2AX-positive cells when compared with infected WT mice (Figure 6A). In addition, $Rnf43^{\Delta Ex8}$ mice showed reduced apoptosis compared with WT mice, as shown by fewer cleaved caspase 3–positive cells in the stomach after infection (Figure 6A).

We also analyzed whether the changes observed in $Rnf43^{\Delta Ex8}$ mice could be related to WNT activation by staining stomach tissue samples of naïve and infected mice for β-catenin. β-catenin expression was up-regulated upon infection in WT as well as in Rnf43 mutant mice, confirming activation of WNT signaling by H $pylori$. However, no differences between wild-type and $Rnf43^{\Delta Ex8}$ mice were observed (Figure 6A).

Together, these results indicate that loss of Rnf43 aggravates H $pylori$–induced inflammation, but at the same time results in reduced DDR. In addition, these effects are independent of alterations in the WNT pathway.

RNF43 Expression Varies During Gastric Carcinogenesis

Our results indicate that H $pylori$ infection induces RNF43 expression, which relates to induction of DDR. To further confirm these observations in human tissue, we analyzed human gastric biopsy specimens from healthy, as well as H $pylori$–infected subjects presenting with gastritis (Table 1). A higher number of RNF43 and γH2AX-positive cells was detected in H $pylori$–positive gastritis compared with healthy mucosa (Figure 7A), confirming that H $pylori$ infection up-regulates RNF43 expression and induces DNA damage in gastric cells. We further analyzed intestinal metaplasia and gastric tumor samples (Table 1), the latter restricted to intestinal- and diffuse-type tumors according to Lauren's[1] classification. Increased expression of RNF43 was observed in all gastric lesions analyzed (Figure 7A). Interestingly, expression of RNF43 correlated to γH2AX levels in intestinal metaplasia (Spearman r_s = 0.7103; P < .0001) as well as in diffuse-type gastric tumors (Spearman r_s = 0.4426; P = .0267) (Figure 7B), although no correlation could be observed in gastritis or intestinal-type gastric tumors (Figure 7B).

RNF43 Mutations Upstream of the RING Domain Confer Resistance to DNA Damage

$RNF43$ was observed to be mutated frequently in gastric tumors. To determine whether our samples carried WT or mutated $RNF43$, we sequenced a subset of intestinal metaplasia (n = 12), intestinal-type (n = 15), and diffuse-type (n = 13) gastric tumors. No mutations in $RNF43$ were detected in intestinal metaplasia samples. Three of the 12 samples analyzed harbored mutations in APC (p.A1471Gfs*14; p.R1463fs; p.R1450X). In 2 cases, APC mutation co-occurred with a mutation in $BRAF$ (p.N581S) and $KRAS$ (p.G13D), respectively. Mutated $ERBB4$ (p.L713V) was observed in 1 of the intestinal metaplasia cases (Table 2).
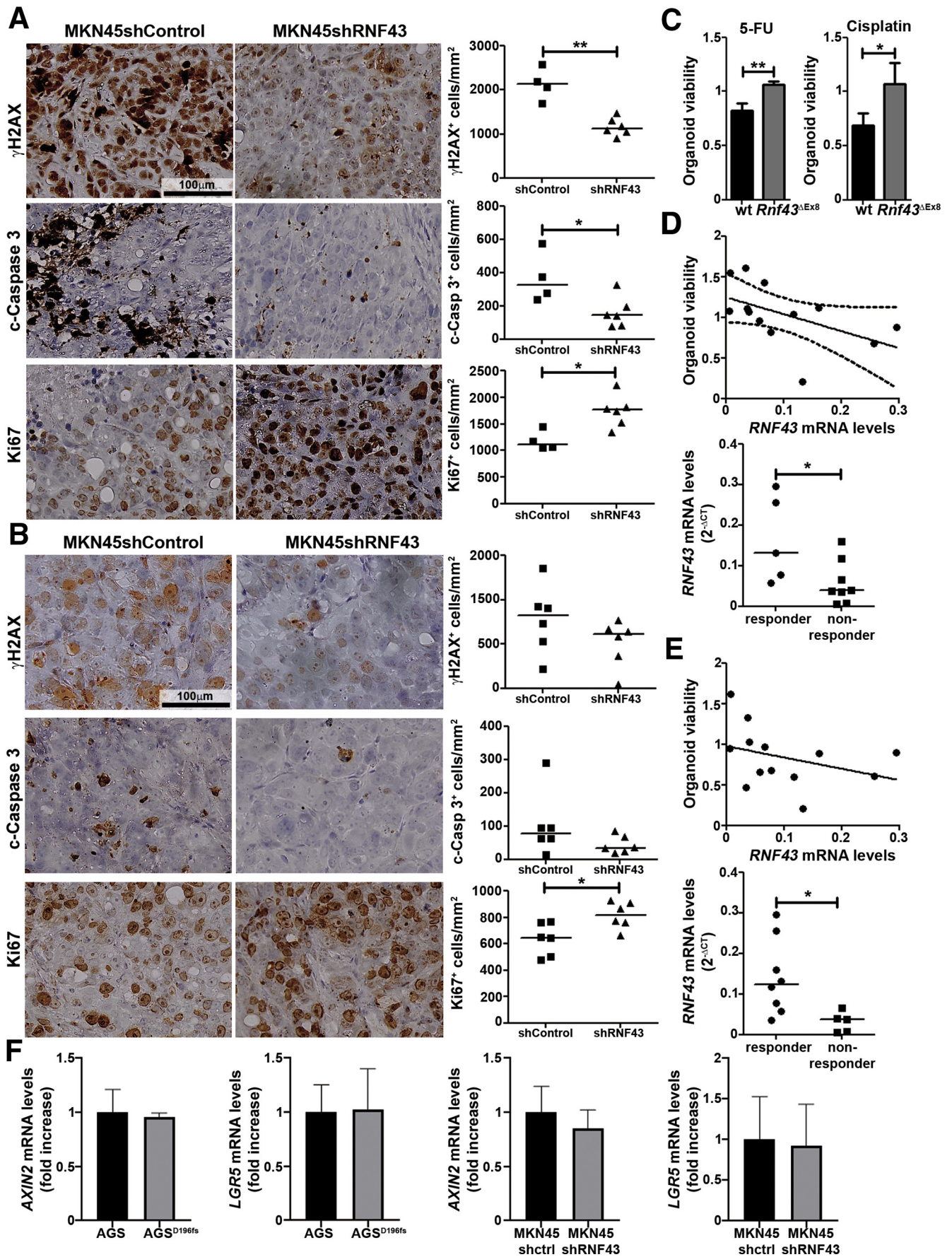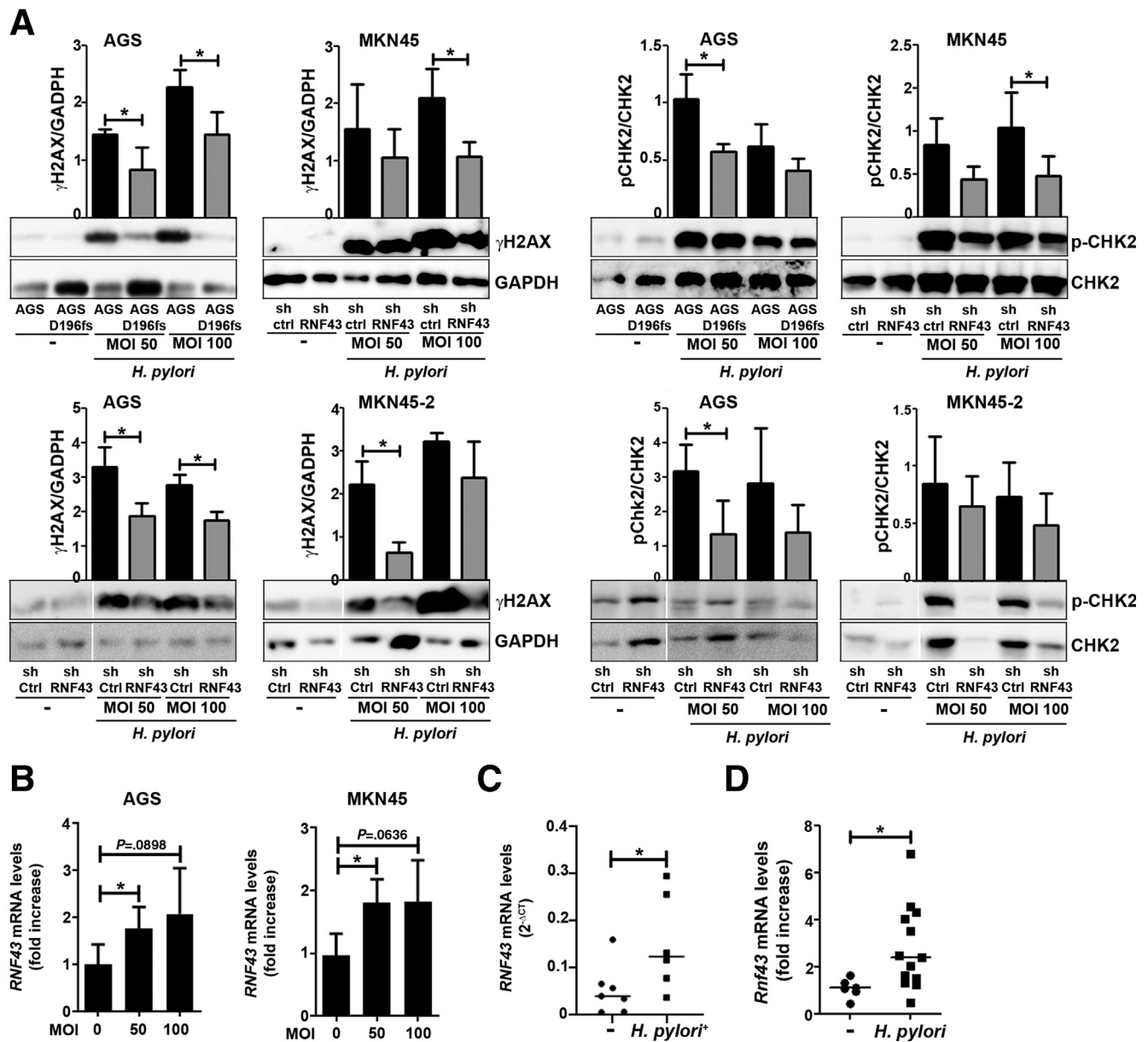
Figure 5. RNF43 is involved in *H pylori*–induced DDR. (*A*) Western blot analysis and quantification of γH2AX and CHK2 expression in WT AGS, AGS[D196fs], control MKN45 and AGS (shCtrl), and RNF43 knockdown MKN45 and AGS (shRNF43) cells upon *H pylori* PMSS1 infection at different multiplicity of infection (MOI). GAPDH was used as a loading control (N = 4). (*B*) *RNF43* mRNA levels after *H pylori* infection of AGS and MKN45 cells. Cycle threshold (C$_T$)values were normalized to *GAPDH* and fold change was calculated over uninfected cells (N = 4). (*C*) *RNF43* mRNA levels normalized to *GAPDH* in gastric biopsy specimens from uninfected (n = 6) and *H pylori*–infected (n = 6) subjects. (*D*) *Rnf43* mRNA levels in the stomach of WT mice (n = 13) after 3-month *H pylori* PMSS1 infection. C$_T$ values were normalized to *Gapdh* and fold change was calculated over uninfected mice (n = 6). Error bars indicate SD. *P ≤ .05, (*A* and *B*) 2-tailed unpaired *t* test, (*C* and *D*) Mann–Whitney test. GAPDH, glyceraldehyde-3-phosphate dehydrogenase; mRNA, messenger RNA.

Figure 4. (*See previous page*). **RNF43 influences susceptibility to DNA damage-inducing chemotherapeutics.** Representative images showing γH2AX, cleaved caspase 3 (c-caspase 3), and Ki67 detected by immunohistochemistry in xenograft tumors that originated from control MKN45 (shCtrl) and RNF43 knockdown MKN45 (shRNF43) cells after treatment with (*A*) 5-fluorouracil or (*B*) cisplatin. Quantification of positive cells per square millimeter is shown. Each *dot* represents 1 mouse. (*C*) Viability of gastric organoids from WT or *Rnf43*[ΔEx8] mice after treatment with 5-fluorouracil (5-FU) or cisplatin. Values were normalized over untreated (N = 3). Spearman correlation between *RNF43* mRNA expression levels in human gastric tissue samples (N = 13), and viability of organoids generated from the same tissue samples after treatment with (*D*) 5-fluorouracil or (*E*) cisplatin. *RNF43* mRNA levels normalized to *GAPDH* also are shown. (*F*) *AXIN2* and *LGR5* mRNA levels in AGS, AGS[D196fs], and MKN45 control and RNF43 knockdown cells. Cycle threshold (C$_T$)values were normalized to *GAPDH* and fold change was calculated over control cells (N = 3). Error bars indicate SD. *Horizontal lines* represent the median values. *P ≤ .05, **P ≤ .01, (*C* and *F*) 2-tailed unpaired *t* test, (*A*, *B*, *D*, and *E*) Mann–Whitney test. mRNA, messenger RNA.

Mutations in *RNF43* were found only in gastric tumors. Two of the intestinal-type gastric tumors carried mutated *RNF43* (p.D628G and p.R371R; p.R132X). Interestingly, 5 of the 15 cases analyzed presented mutations in *TP53*. *RNF43* was mutated in 2 diffuse-type tumors (p.R584fs; p.R132X). In this subset of tumors, mutations in *CDH1* were the most
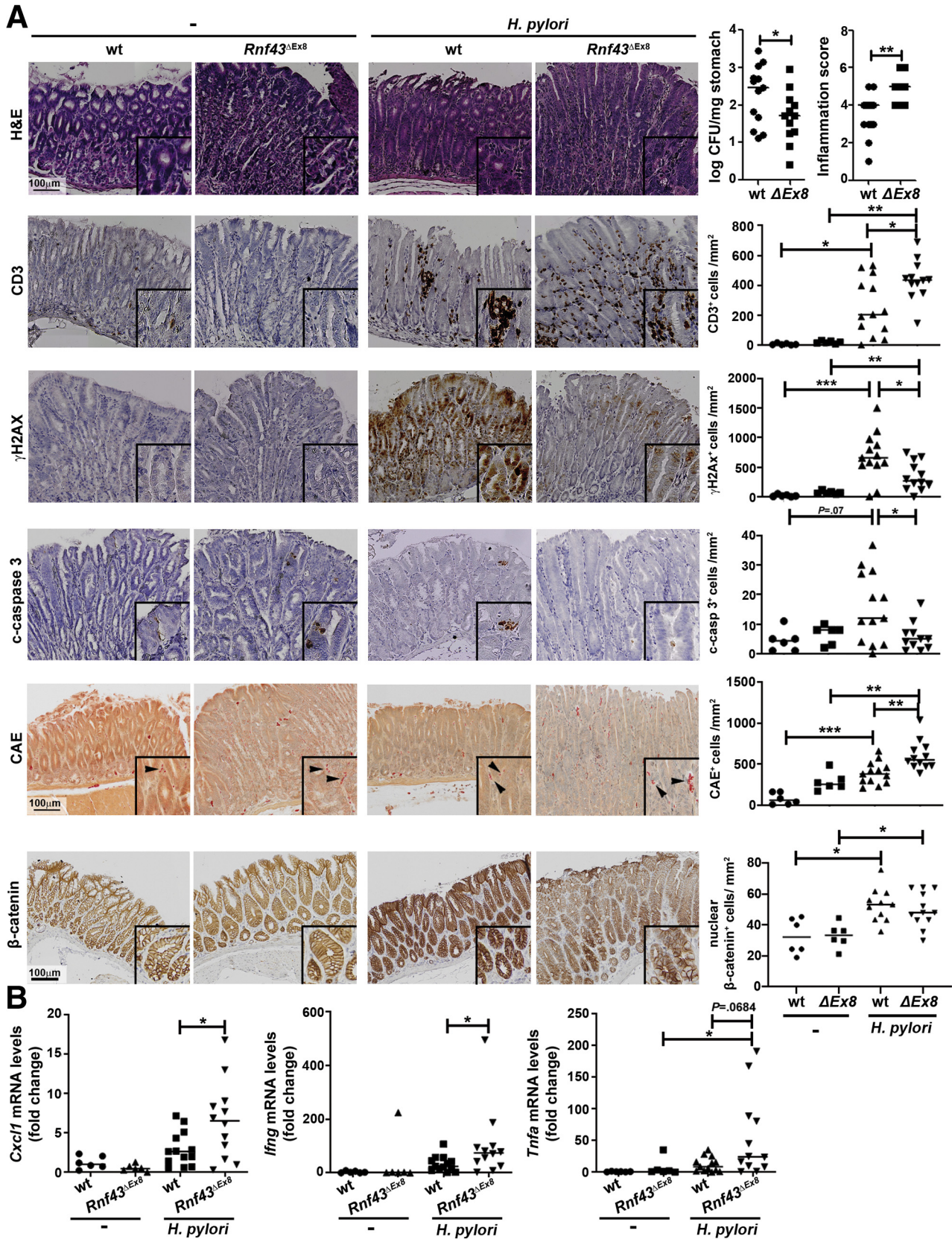
frequent (4 of 13 cases), as expected for this type of stomach cancer. A summary of the mutations can be found in Table 2. RNF43 mutations have been found more frequently in MSI-high tumors. Mutated diffuse-type tumors were genomically stable, as expected.[3] In contrast, 1 of the intestinal-type tumors carrying mutated RNF43 was MSI-high (Table 2).

In most of the cases analyzed we found single-nucleotide polymorphism (SNP) variants of *RNF43*, namely I47V (rs3744093), R117H (rs2257205), L418M (rs2526374), and P686R (rs9652855) (Table 2). It recently was shown that a SNP of the *RNF43* X117 site is associated with overall survival of colorectal cancer patients.[29] To determine whether this could be related to an altered response to DNA damage-inducing chemotherapy, we sequenced human gastric organoids to identify SNPs and analyzed their response to 5-fluorouracil and cisplatin. Five SNPs were found frequently. The I47V variant was found in 23 of the 40 cases (57.5%). Nine cases carried the R117H variant (22.5%). The L418M variant was observed in 18 cases (45%), and the P686R variant was observed in 7 cases (17.5%). In 6 cases (15%) we found the variant R343H (rs34523089), which was detected in only 2 tumor samples (Table 2). No difference in response to chemotherapy was detected between samples harboring WT *RNF43* and samples presenting any of the aforementioned SNPs (Figure 8A).

To determine whether mutations occurring in tumors conferred resistance to γ-radiation, we selected 2 mutations observed in our tumor cohort and generated AGS cells carrying these mutations by CRISPR/CAS9 editing. We selected mutations occurring before (p.R132X) or downstream of the RING domain (p.R584fs). After transfection of guide RNAs we could not introduce the indicated mutations but obtained cells carrying the frameshift mutations A136fs and Q577fs, respectively. Because these mutations give rise to similar proteins, we used the generated AGS^A136fs and AGS^Q577fs in further experiments. AGS^A136fs cells showed resistance to γ-radiation as more colonies were observed (Figure 8B). In contrast, AGS^Q577fs cells were as sensitive to γ-radiation as WT cells. Similarly, the frameshift mutation A136fs conferred increased resistance to chemotherapy in AGS cells (Figure 8C), while the viability of cells expressing the Q577fs mutation after 5-fluorouracil or cisplatin treatment was similar to the viability of AGS WT cells.

These findings show that mutations upstream of the RING domain of RNF43 in gastric cells confer resistance to DNA damage-inducing agents, and confirm the importance of the RING domain for proper function of the protein.

RNF43 Regulates DNA Damage Response by Ubiquitinating γH2AX

We finally explored the molecular mechanism by which RNF43 regulates DDR. We observed that upon induction of DNA damage, RNF43 co-localized with γH2AX in the nucleus of irradiated cells (Figure 9A and B). Moreover, direct interaction between RNF43 and γH2AX was detected in co-immunoprecipitation experiments after irradiation of AGS cells (Figure 9C).

We next analyzed whether RNF43 influenced γH2AX ubiquitination status. To this end, we immunoprecipitated γH2AX in AGS^D196fs and MKN45shRNF43 cells and detected K48 and K63 ubiquitination by Western blot. We observed that ubiquitination of γH2AX was reduced in RNF43-depleted cells (Figure 9D), indicating that RNF43 is involved in DDR by interacting and ubiquitinating γH2AX.

Discussion

Several studies have shown that *RNF43* is mutated in tumors of the gastrointestinal tract, including colorectal, pancreatic, and GC. *RNF43* mutations found in GC were considered driving mutations of gastric carcinogenesis,[8] occurring early during transition of adenomas to carcinomas.[30] Functionally, the importance of RNF43 for tissue homeostasis derives from its role as an inhibitor of the WNT signaling pathway.[14,15] However, our previous data suggest that the tumor-suppressor activity of RNF43 in gastric cells is independent of WNT. In a xenograft model using human gastric epithelial cells with lentiviral-mediated silencing of RNF43, we observed no changes in the activation of WNT signaling. In addition, gastric alterations detected in *Rnf43*^ΔEx8 mice were not related to changes in the expression of WNT target genes,[13] indicating that RNF43 might have an alternative function in the stomach. Interestingly, various RING finger proteins have been reported to play important roles in DDR by ubiquitinating the central histone H2AX. For instance, a complex of RNF2 and RNF51 ubiquitinates γH2AX at the lysine residues K118/K119,[31] while RNF8 and RNF168 attach further K63-linked ubiquitin chains to this histone.[17,18,32] RNF168 also has been described to ubiquitinate γH2AX at the lysine residues K13/K15, which has been shown to be important for DDR signaling.[33] In our study, we observed that loss of RNF43 function resulted in reduced levels of K63- and K48-linked γH2AX ubiquitination upon irradiation, which translated into impaired DDR activation and enhanced cellular survival. These results indicate an important role of RNF43 in DDR because ubiquitination of γH2AX has been described

---

Figure 6. (*See previous page*). **RNF43 is involved in *H pylori*–induced DDR.** (*A*) Colony forming units (CFU)/mg of stomach of WT (n = 13) and *Rnf43*^ΔEx8 mice (n = 12), and inflammatory score after *H pylori* infection. Activity and chronicity were evaluated in antrum and corpus according to the updated Sydney system. Representative images and quantification of CD3, γH2AX, cleaved-caspase 3 (c-casp3), chloroacetate esterase (CAE)-positive cells (neutrophils and mast cells), and nuclear β-catenin–positive cells per square millimeter of tissue stained by immunohistochemistry in murine gastric tissue samples are shown. *Arrowheads* indicate positive cells. (*B*) *Cxcl1*, *Ifng*, and *Tnfa* mRNA levels in the stomach after 3-month *H pylori* PMSS1 infection. Cycle threshold (C_T)values were normalized to *Gapdh* and fold change was calculated over uninfected mice. *Horizontal lines* represent the median values. *P ≤ .05, **P ≤ .01, and ***P ≤ .001, Mann–Whitney test. mRNA, messenger RNA.

Table 1. List of Human Gastric Biopsy Specimens Classified by Gastric Pathology Observed

Sample ID	Sex	Age, y	H pylori status
Healthy stomach			
H1	M	76	Negative
H2	M	55	Negative
H3	F	90	Negative
H4	F	80	Negative
H5	F	39	Negative
H6	M	72	Negative
H7	F	84	Negative
H8	M	59	Negative
H9	M	69	Negative
H10	M	27	Negative
H11	F	62	Negative
H12	M	59	Negative
H13	M	72	Negative
H14	M	33	Negative
H15	F	50	Negative
H16	F	24	Negative
H17	F	27	Negative
H18	F	41	Negative
H19	F	22	Negative
H20	F	27	Negative
Gastritis			
G1	M	60	Positive
G2	M	57	Positive
G3	M	59	Positive
G4	F	60	Positive
G5	F	32	Positive
G6	M	58	Positive
G7	F	85	Positive
G8	F	73	Positive
G9	M	90	Positive
G10	F	83	Positive
G11	F	72	Positive
G12	F	78	Positive
G13	F	82	Positive
G14	M	60	Positive
G15	M	90	Positive
G16	M	91	Positive
G17	M	47	Positive
G18	F	48	Positive
G19	F	32	Positive
G20	M	74	Positive
G21	F	81	Positive
G22	F	52	Positive
G23	M	90	Positive
G24	M	68	Positive
Intestinal metaplasia			
IM1	M	76	Eradicated
IM2	M	81	Negative
IM3	F	67	Eradicated
IM4	F	80	Negative
IM5	F	68	Eradicated
IM6	M	55	Eradicated
IM7	M	31	Eradicated
IM8	M	63	Eradicated
IM9	F	80	Eradicated
IM10	M	40	Eradicated
IM11	M	67	Eradicated
IM12	F	84	Positive
IM13	F	85	Eradicated
IM14	F	66	Eradicated
IM15	M	75	Eradicated
IM16	M	75	Eradicated
IM17	M	64	Negative
IM18	F	82	Eradicated
IM19	F	52	Eradicated
IM20	M	86	Positive
IM21	F	64	Eradicated

Table 1. Continued

| Sample ID	Sex	Age, y	H pylori status
IM22	M	76	Positive
IM23	F	54	Positive
IM24	F	33	Eradicated
IM25	M	61	Negative
IM26	M	86	Eradicated
IM27	M	68	Eradicated
Intestinal-type gastric cancer			
GCi1	F	80	Negative
GCi2	F	57	Positive
GCi3	M	71	Eradicated
GCi4	M	87	Eradicated
GCi5	F	78	Negative
GCi6	M	66	Negative
GCi7	M	53	Positive
GCi8	F	82	ND
GCi9	F	79	Positive
GCi10	M	72	Negative
GCi11	M	86	Negative
GCi12	F	79	Eradicated
GCi13	M	88	Negative
GCi14	F	77	Eradicated
GCi15	F	82	ND
GCi16	M	70	0
GCi17	M	70	Positive
GCi18	F	95	Positive
GCi19	M	88	Negative
GCi20	F	98	ND
GCi21	M	86	Negative
GCi22	M	62	ND
GCi23	F	58	ND
GCi24	M	86	Eradicated
GCi25	M	73	Eradicated
GCi26	F	80	Negative
GCi27	F	98	Positive
GCi28	M	82	ND
GCi29	F	95	Eradicated
GCi30	F	84	Eradicated
Diffuse-type gastric cancer			
GCd1	F	86	Negative
GCd2	F	77	Eradicated
GCd3	M	71	Eradicated
GCd4	F	75	Eradicated
GCd5	M	69	Negative
GCd6	M	77	Eradicated
GCd7	F	81	Negative
GCd8	F	82	Negative
GCd9	F	58	ND
GCd10	M	98	ND
GCd11	F	83	ND
GCd12	M	82	Negative
GCd13	F	94	ND
GCd14	M	89	Positive
GCd15	F	87	Eradicated
GCd16	F	86	Eradicated
GCd17	M	76	Positive
GCd18	M	34	Eradicated
GCd19	M	85	ND
GCd20	M	51	Positive
GCd21	M	72	Negative
GCd22	M	51	ND
GCd23	F	85	Negative
GCd24	F	91	Eradicated
GCd25	F	81	Negative
GCd26	F	78	Positive

ND, not determined.
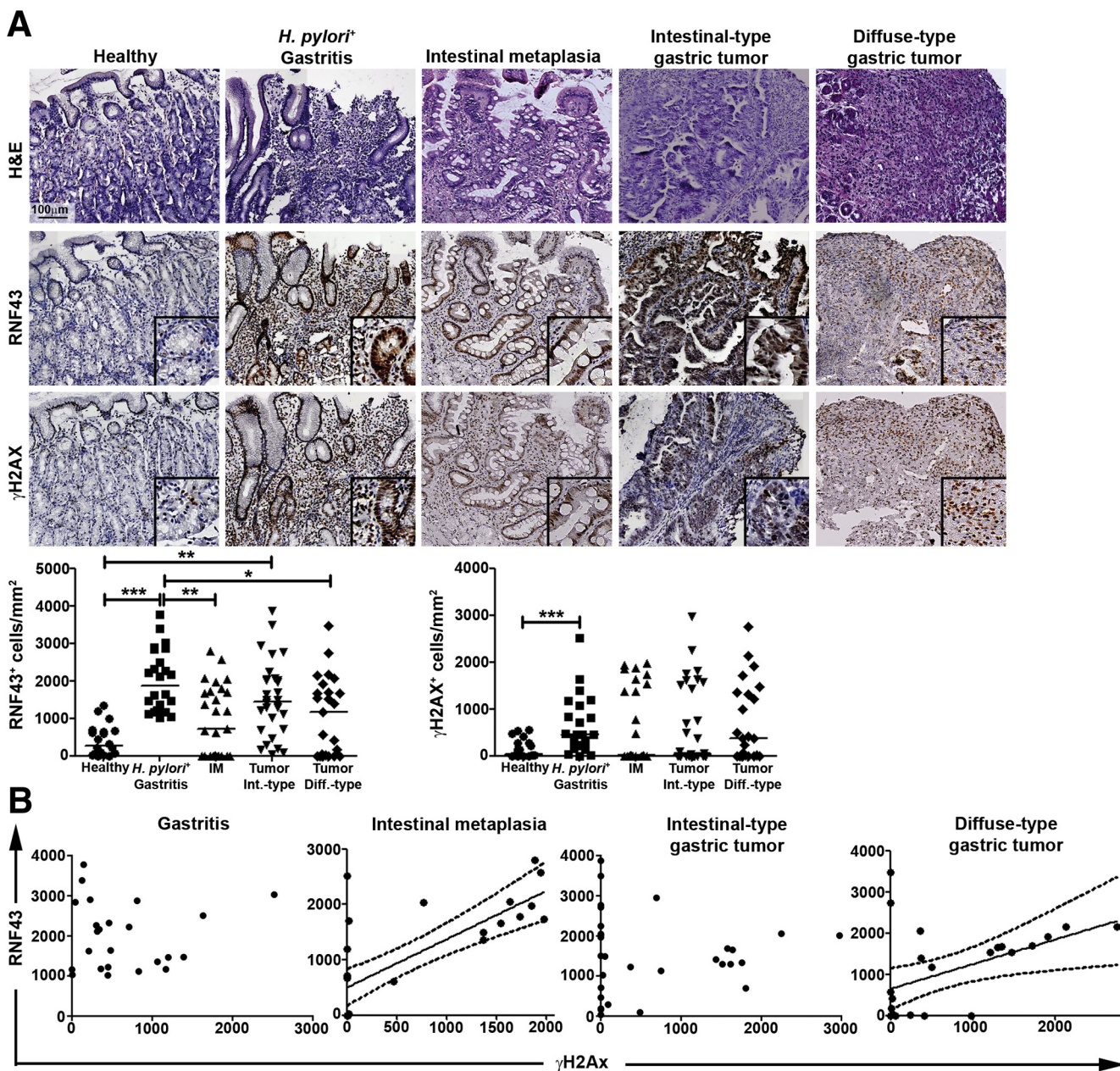
Figure 7. RNF43 expression varies during gastric carcinogenesis. (*A*) Representative images and quantification of RNF43 and γH2AX-positive cells per square millimeter of human gastric tissue of healthy individuals (n = 20), and patients with gastritis (n = 24), intestinal metaplasia (n = 27), and intestinal-type (n = 20) or diffuse (n = 25) gastric cancer. *Horizontal lines* represent the median values. Each *dot* represents 1 sample. $*P \leq .05$, $**P \leq .01$, and $***P \leq .001$, 1-way analysis of variance multiple comparisons. (*B*) Spearman correlation between the number of RNF43 and γH2AX-positive cells per square millimeter of human gastric tissue. Diff, diffuse; IM, intestinal metaplasia; Int, intestinal.

extensively as a central post-translational modification for the initiation[19,34] and maintenance[17,18,33] of DDR signaling.

The expression of RNF43 was found to be increased upon DNA damage. Top transcription factor binding sites described in the *RNF43* gene promoter include aryl hydrocarbon receptor (AhR), Activator protein 1 (AP-1), Aryl Hydrocarbon Receptor Nuclear Translocator (Arnt), c-Fos Proto-Oncogene, AP-1 Transcription Factor Subunit (c-Fos), c-Jun Proto-Oncogene, AP-1 Transcription Factor Subunit (c-Jun), Forkhead Box O4 (FOXO4), and Peroxisome

Proliferator Activated Receptor Gamma (PPAR-γ) (Gene-Cards). All of these transcription factors have been implicated in different aspects of the DDR, and therefore could be regulating RNF43 expression upon DNA damage. The identification of the transcription factors involved and the regulatory mechanisms behind it require further investigation.

H pylori infection is the main risk factor for GC development. Previous studies have indicated that *H pylori* can induce DNA damage directly to host cells through interaction of the type IV secretion system with integrin β1. This

Table 2. List of Mutations Found in Human Gastric Tissue Samples

Sample	RNF43 SNPs	RNF43 mutations	Other mutations	MSI status
Intestinal metaplasia				
IM1	p.I47V p.R117H p.P686R	–	APC p.A1471Gfs*14 BRAF p.N581S	
IM2	p.I47V p.R117H	–	APC p.R1445fs KRAS p.G13D	
IM3	p.R117H p.P686R	–	–	
IM4	–	–	ERBB4 p.L713V	
IM5	p.I47V p.R117H p.L418M	–	APC p.R1432X	
IM6	p.R117H p.P686R	–	–	
IM7	p.R117H	–	–	
IM8	p.I47V p.L418M p.P686R	–	–	
IM9	p.R117H p.L418M	–	–	
IM10	p.I47V	–	–	
IM11	p.R117H	–	–	
IM12	p.I47V p.R117H p.L418M	–	–	
Intestinal-type gastric cancer				
GCi1	p.I47V p.R117H p.L418M	–	PTPRT p.P1075Rfs PIK3CA p.E542K TLR4 p.L10M	
Gci2	p.P686R	–	ERBB2 p.V842I	MSS
Gci3	p.R117H p.P760P	–	MDM2 amplification	
Gci4	–	–	Sox2 p.E36G APC p.R1432X PREX2 p.L50V TP53 p.G66R	
Gci5	p.I47V p.R117H p.L418M	–	TP53 p.E204X	
Gci6	p.I47V p.L418M p.P686R	–	TP53 p.R116Q TP53 p.Y88H CDKN2A p.Q50H	
Gci7	p.I47V p.R117H	–	TLR4 p.L298V PTPRT p.E911G	
Gci8	p.I47V p.L418M p.P686R	–	ARID1A p.P1467fs PTEN M134T TP53 R151H	
Gci9	WT	–	–	
Gci10	p.I47V p.L418M	–	–	MSS
Gci11	p.I47V p.R343H p.L418M	–	CDKN2A p.Q70X PTEN p.R130X TGFBR2 p.D405N	
Gci12	R117H	–		MSS
Gci13	p.I47V p.L418M	–	TP53 p.G134E APC p.R1432X	
Gci14	p.I47V p.R117H	p.R371R p.D628G	CCND1 p.S257P	MSS
Gci15	–	p.R132X	FBXW7 p.A508D RHOA p.Y42C ARID1A p.P2095fs	MSI

Table 2. Continued

Sample	RNF43 SNPs	RNF43 mutations	Other mutations	MSI status
Diffuse-type gastric cancer				
GCd1	p.I47V p.L418M	–	PREX2 p.R186Q	
GCd2	p.I47V p.R117H p.P686R	–	–	
GCd3	–	p.R584fs	ERBB2 p.R678Q CDH1 p.E429G	MSS
GCd4	p.I47V p.L418M	–	–	MSS
GCd5	p.L418M	–	CDH1 p.D254H	
GCd6	p.I47V p.L418M	–	–	
GCd7	–	p.R132X	TP53 p.R117M	MSS
GCd8	p.I47V p.R343H p.L418M	–	ARID1A p.R2158L CDH1 c.531+1G>T	MSS
GCd9	p.I47V p.L418M	–	CDH1 p.E243K	MSS
GCd10	p.I47V p.L418M	–	KRAS p.G13D TP53 p.R150W PIK3CA p.N345K PIK3CA p.A1066V MTOR p.R2317I	
GCd11	p.P686R	–	–	
GCd12	p.I47V p.L418M	–	–	
GCd13	p.I47V p.L418M	–	PIK3CA p.H1047R	

MSS, microsatellite stable.

interaction would lead to the activation of nuclear factor-κB signaling and thereby to the activation of nucleotide excision repair endonucleases responsible for inducing DSBs.[26] In contrast, the involvement of other virulence factors such as vacuolating cytotoxin A (VacA) in the induction of DSBs was excluded.[25] Whether these virulence factors play a role in the RNF43-mediated DDR therefore deserves further investigations.

Current treatment of GC patients includes adjuvant chemotherapy with cisplatin or 5-fluorouracil, as well as irradiation.[35] The efficacy of these treatments to eliminate tumor cells is based on their ability to induce DNA damage. However, not all tumors respond to adjuvant therapy, and biomarkers that could predict response still are lacking. In a previous study, overexpression of RNF43 was shown to render gastric cells more susceptible to oxaliplatin and 5-fluorouracil, but the molecular mechanisms involved remained unclear.[36] In line with this observation, we also found that loss of RNF43 function confers resistance to DNA damage-inducing chemotherapy. More importantly, we identified the mechanism responsible, namely the direct role of RNF43 in DDR.[36]

Furthermore, we observed a correlation between response to chemotherapy and RNF43 expression levels in human gastric organoids, indicating that not only loss of functional protein but also its down-regulation or up-regulation might modify resistance to DNA damage-inducing chemotherapeutics. We postulate that treating

patients expressing low levels of RNF43, or carrying mutations affecting its functional domain, with DNA-damaging drugs and radiation therapy (as recommended in the guidelines[28]) would lead to detrimental effects. Thus, cells lacking RNF43 not only would resist radiotherapy or chemotherapy-induced apoptosis, but eventually would accumulate additional mutations induced by the treatments themselves, contributing to tumor progression and thereby worsening prognosis. Along these lines, decreased RNF43 expression has been associated with distant metastasis, TNM stage, and poorer overall survival of GC patients,[36] supporting our hypothesis. It also is relevant to note that *RNF43* mutations are highly enriched in MSI gastric tumors,[8,11,12,30] which are characterized by a high mutation burden in tandem repeats[37] caused by deficient DNA repair machinery.[38] Therefore, it is plausible that acquired mutations in *RNF43* may contribute to the increased mutation rate in MSI tumors by further impairing DDR activation.

Our data suggest that mutations downstream of the catalytic domain of RNF43 still would retain functionality. This observation is in line with recent data showing that, for instance, the most common RNF43 mutation in gastric tumors (G659Vfs*41) is still fully functional in terms of WNT inhibition.[39]

In light of our findings, the inclusion of *RNF43* in GC gene panels for the screening of patients should be considered to select therapeutic regimens based on mutation status. This,
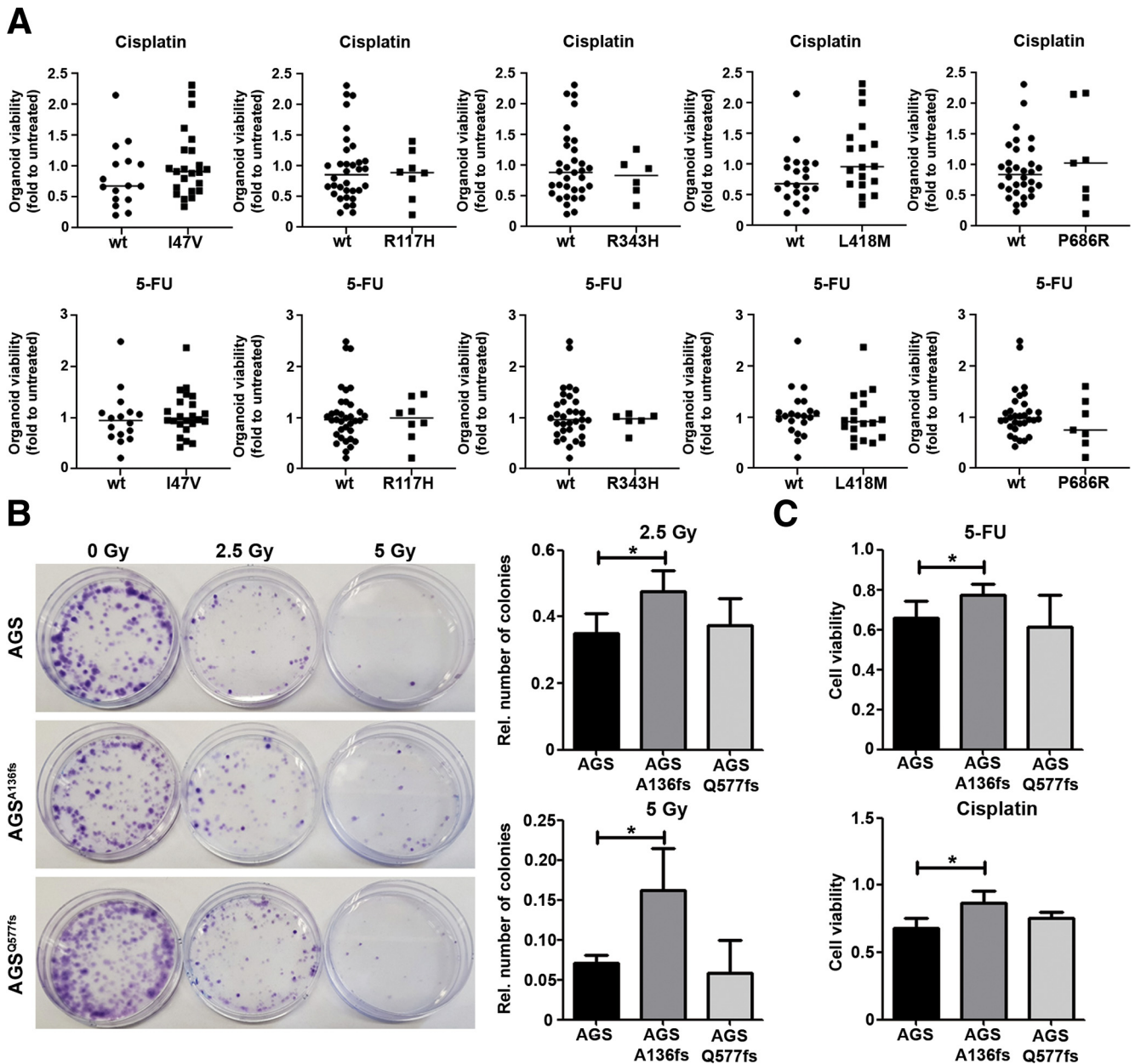
Figure 8. RNF43 mutations upstream of the RING domain confer resistance to DNA damage. (*A*) Viability of gastric organoids (n = 40) carrying different SNP variants of *RNF43* after treatment with 5-fluorouracil (5-FU) or cisplatin. Fold change was calculated over untreated organoids. *Horizontal lines* represent the median values. Mann–Whitney test. (*B*) Representative images and quantification of cell colonies after γ-radiation. (n = 4). (*C*) Cell viability after treatment with 5-FU or cisplatin. Values were normalized over untreated cells (n = 4). Error bars indicate SD. *$P \le .05$, 2-tailed unpaired *t* test. Rel, relative.

together with the examination of protein expression levels of WT RNF43, may serve as a biomarker for therapy selection for GC patients. Moreover, screening of *RNF43* mutations and expression also could be considered for other types of tumors such as colorectal or pancreatic cancers, where mutations in *RNF43* have been observed frequently. In fact, and as mentioned earlier, a possible role of RNF43 in DDR in pancreatic cells already has been suggested.[40] As such, further investigations in other tissues will be important to confirm a general function of RNF43 as a modulator of DDR.

Materials and Methods
Cell Culture and Cell Treatments

AGS (ATCC CRL-1739) and MKN45 (RCB1001) cells were cultured in Dulbecco's modified Eagle medium (Invitrogen, Carlsbad, CA) containing 10% fetal calf serum (Sigma-Aldrich, St. Louis, MO) at 37°C in a humidified atmosphere (5% CO_2). Cells were tested routinely for *Mycoplasma* contamination. Short tandem repeat analysis was performed for authentication of the cell lines used. AGS and MKN45 shControl and shRNF43 cells were generated using

lentiviruses as previously described.[13] Sequences are listed in Table 3.

AGS^{D196fs}, AGS^{A136fs}, and AGS^{Q577fs} cells were generated by CRISPR/Cas9. To generate AGS^{D196fs} cells, we used guide RNAs targeting exon 6 of *RNF43* to introduce a 4-bp deletion at aspartic acid 196. The resulting frameshift mutation leads to a premature stop codon 5 amino acids downstream, deleting the functional RING
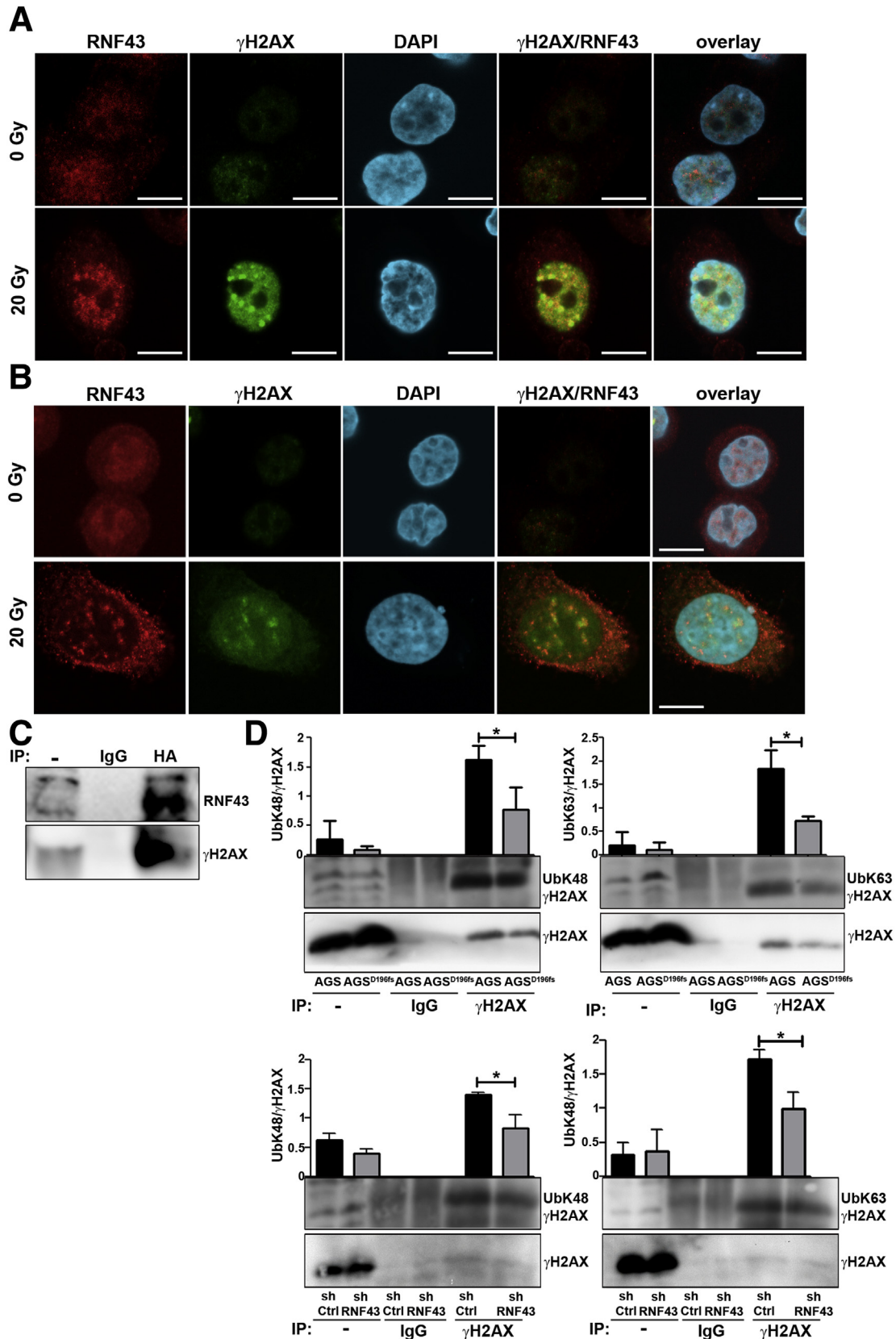
Table 3. DNA-Oligo Sequences for Lentiviral Knockdown and CRISPR/Cas9 Editing

Oligo	Forward	Reverse
shRNF43 1	GGAGAAAGCTATTGCACAGAA	TTCTGTGCAATAGCTTTCTCC
shRNF43 2	CGCGTCCCCTTCTTGGTAAGATC GAGAGTTCAAGAGACTCTCGATCTT ACCAAGAATTTTTGGAAAT	CGATTTCCAAAAATTCTTGGTAAGAT CGAGAGTCTCTTGAACTCTCGATCT TACCAAGAA GGGGA
shctrl 1	GCAACTTCAGCTATATCATTT	AAATGATATAGCTGAAGTTGC
shctrl 2	CGCGTCCCCGTACAGCCGCCTCAATTCT TTCAAGAGAAGAATTGAGGCGGCTGT ACTTTTTGGAAAT	CGATTTCCAAAAAGTACAGCCGCCTCA ATTCTTCTCTTGAAAGAATTGAGGCGGCT GTACGGGGA
Guide RNA CRISPR/Cas9 AGS^D196fs	CCACACATCATAATCTGGCT	AGCCAGATTATGATGTGTGG
Guide RNA CRISPR/Cas9 AGS^R132X	GATGTCAAAGAGGACAGCAC	–
Guide RNA CRISPR/Cas9 AGS^R584fs	AAACCGGAGTCCCCCAGTCC	–

domain. Guide RNA sequences (Table 3) were designed using www.tools.genome-engineering.org, annealed, and cloned into a pX330 vector (42230; Addgene, Watertown, Massachusetts, USA) containing green fluorescent protein (GFP). Cells were transfected with Lipofectamine 2000 (Invitrogen), sorted for GFP, and grown as single-cell colonies. Genomic DNA was extracted using the Pure-Link Genomic DNA Mini Kit (Invitrogen), and mutations in *RNF43* and selected off targets were checked by Sanger sequencing.

For targeted mutations, Cas9 ribonucleoproteins (RNPs) were transfected together with an oligonucleotide containing the desired mutations and homology arms flanking 30 bp of the site of interest on both sides. Guide RNA and repair oligonucleotides were planned using Benchling (www.benchling.com), and guide RNAs, ATTO 550-labeled tracer RNA, and Cas9 protein were purchased from Integrated DNA Technologies (Coralville, IA). Repair oligonucleotides were purchased as single-stranded DNA, as follows:

R132X: *TGCCTCTGCAGGCTCGGATGGCGGGTGAGTG AGGAGCAAGTGCTGTCCTCTTTGACATCA*;

R584fs: *CAGAAACCGGAGTCCCCCAGTCCAGAC CTCCTATTCCTCGACACAGCCCCAGCCAGAGCCACCTTCTCCT*.

RNP assembly and transfection were performed as described by Integrated DNA Technologies. AGS cells ($5*10^5$) were electroporated with RNPs using a Nucleofector 4D (Kit X, pulse code DS-135; Lonza, Basel, Switzerland). To increase homology-directed repair, Nu7026 (20 μmol/L; Sigma-Aldrich) and Trichostatin A (0.01 μmol/L; Sigma-Aldrich) were added. At 24 hours after electroporation, cells were sorted for ATTO 550 and seeded as single-cell clones for selection.

Lipofectamine 2000 (Invitrogen) was used for plasmid transfections. Transfected cells were cultured for 36 hours before being subjected to γ-radiation and subsequent co-immunoprecipitation.

γ-radiation was performed using a Cs^{137} radiation source (Buchler, Braunschweig, Germany). For chemotherapeutic treatment, cells were seeded in a 96-well plate (7500 cells/well) and treated with 5-fluorouracil (2 μg/mL) or cisplatin (10 μg/mL) for 48 hours, followed by measurement of cell viability using Cell-counting kit 8 (Sigma-Aldrich).

Cell Viability and Clonogenicity Assay

AGS and MKN45 cells were seeded in a 96-well plate (2500 cells/well) after γ-radiation, and serum-starved for 24 hours. After addition of serum-containing medium, cells were allowed to grow for 48 hours and cell viability was measured using Cell-counting kit 8 (Sigma-Aldrich).

To assess clonal expansion, AGS and MKN45 cells were irradiated and seeded at low density. After 14 days, single-cell colonies were fixed and stained with 6% glutaraldehyde containing Crystal Violet.

Annexin V Staining

Four days (AGS) or 6 days (MKN45) after γ-radiation, cells were stained with Annexin V Pacific Blue conjugate (Invitrogen) and propidium iodide (Sigma-Aldrich). Fluorescence was measured in a CyAn ADP flow cytometer (Beckmann Coulter, Brea, CA) and analyzed with FlowJo (Becton, Dickinson & Company, Franklin Lakes, NJ).

H pylori *Infection*

H pylori strain PMSS1[41] was cultured on Wilkins-Chalgren Dent agar plates in a microaerophilic atmosphere.

Figure 9. (*See previous page*). **RNF43 is up-regulated in response to DNA damage and it is recruited to sites of DNA damage.** Representative immunofluorescence images of RNF43 (red) and γH2AX (green) in control and irradiated (*A*) AGS and (*B*) MKN45 cells. *Scale bars*: 10 μm. (*C*) Immunoprecipitation of RNF43 (human influenza hemagglutinin, HA) from AGS cells transfected with HA-tagged RNF43 upon γ-radiation (20 Grey), followed by Western blot analysis (n = 3; 1 representative experiment is shown). (*D*) Immunoprecipitation of γH2AX from AGS and MKN45 cells after radiation (20 Grey), followed by Western blot analysis. -, whole lysate. Quantification of ubiquitinated γH2AX from total γH2AX is shown (n = 3). Error bars indicate SD. *$P \le$ .05, 2-tailed unpaired *t* test. DAPI, 4′,6-diamidino-2-phenylindole; IP, immunoprecipitation.

Table 4. Sequences of the Primers Used in This Study

Primer	Human Forward	Human Reverse	Murine Forward	Murine Reverse
GAPDH	GAAGGTGAAGGTCGGAGT	GAAGATGGTGATGGGATTTC	GCCTTCTCCATGTGGTGAA	GCACAGTCAAGGCCGAGAAT
RNF43 (qPCR)	GAGTGTGCTCCAGATGTGTT	AGTCCTCTTCCA GTCCTTCTA	GGGGCAAACTATGACGTGTG	CTGCTGAAGAGAGATCCGGTC
AXIN2	CTC CCC ACC TTG AAT GAA GA	GTT TCC GTG GAC CTC ACA CT		
LGR5	TGA TGA CCA TTG CCT ACA C	GTA AGG TTT ATT AAA GAG GAG AAG		
Ifng	–	–	TCAAGTGGCATAGATGTGGAAGAA	TGGCTCTGCGCAGGATTTCATG
Cxcl1	–	–	TGCACCCAAACCGAAGTCAT	TTGTCAGAAGCCAGCGTTCAC
TNFα	–	–	CGATGGGTTGTACCTTGTC	CGGACTCCGCAAAGTCTAAG

Cells were infected at a multiplicity of infection (MOI) of 50 and 100 (OD$_{600}$ $1 = 2*10^8$ bacteria/mL) for 24 hours, and lysed in sodium dodecyl sulfate (SDS) sample buffer or RNA lysis buffer.

Quantitative Polymerase Chain Reaction

GenElute Mammalian Total RNA Miniprep Kit (Sigma-Aldrich) was used to isolate RNA. Mouse tissue was homogenized using a Precellys (Bertin Instruments, Montigny-le-Bretonneux, France) lysing kit. MMLV Reverse Transcriptase RNase H−Point Mutant (Promega, Madison, WI) was used for reverse transcription. Transcript abundance was assessed using the GoTaq quantitative polymerase chain reaction Mastermix (Promega) and a CFX384 system (Bio-Rad, Hercules, CA). Primer sequences are included in Table 4. Gene expression was analyzed with the comparative relative expression ($\Delta\Delta C_T$) method.

Immunofluorescence

Cells were seeded on glass coverslips either untreated or immediately after being subjected to γ-radiation (20 Gγ). Immunofluorescence staining was performed as previously described.[13] The monoclonal antibody GGTRNF 8D6 (IgG2b/k) was raised in rats against amino acid residues 329–348 (SRSYQEPGRRLHLIRQHPGH) of human RNF43. Staining was analyzed using a FluoView FV10i confocal microscope (Olympus, Shinjuku, Japan).

Co-immunoprecipitation and Western blot

Cells were lysed in RIPA buffer (50 mmol/L Tris-HCl, pH 7.4, 1% Nonidet P-40 (NP-40), 150 mmol/L NaCl, 0.25% Deoxycholate (DOC), 1 mmol/L ethylene glycol-bis(β-aminoethyl ether)-N,N,N',N'-tetraacetic acid) containing phosphatase and protease inhibitors and precleared using 1 μg appropriate IgG and agarose conjugate. Lysates were centrifuged at 3000 rpm for 1 minute at 4°C, and incubated with primary antibody or IgG overnight at 4°C while rotating. Protein A/G agarose beads (Roche, Basel, Switzerland) were added to the lysates and incubated for 4 hours at 4°C. After washing with phosphate-buffered saline, beads were collected by centrifugation, diluted in SDS sample buffer for Western blot, and boiled for 5 minutes at 95°C.

Protein lysates were subjected to SDS–polyacrylamide gel electrophoresis and transferred to a nitrocellulose membrane. After blocking with 5% low-fat milk in Tris-buffered saline-tween (TBS-T), membranes were incubated in primary antibody (Table 5) overnight at 4°C. Membranes were washed in TBS-T followed by incubation with horseradish peroxidase–conjugated secondary antibodies for 1 hour at room temperature. Signal was visualized using Clarity ECL Western substrate (Bio-Rad) and an Intas chemiluminescence detection system (Intas, Göttingen, Germany).

Gastric Organoids

Gastric organoid culture was established as previously described.[42] There were 100 (48-well plate) or 300 (24-well plate) gastric glands seeded per well.

Table 5. Antibodies Used in This Study

Target	Clone	Assay	Dilution	Company	Reactivity
Annexin V, Pacific Blue conjugate	————————	Flow cytometry	1:100	Thermo Fisher	H, M
(non-p-)β-catenin	D2U8Y	IHC	1:1000	Cell Signaling (Danvers, MA)	H, M
CD3	SP7	IHC	1:150	Thermo Fisher	H, M
Chk2	1C12	WB	1:1000	Cell Signaling	H
Cleaved caspase 3 (Asp175)	9661	IHC	1:300	Cell Signaling	H, M
GAPDH	14C10	WB	1:1000	Cell Signaling	H, M
HA	H6908	IP	1:100	Sigma	–
HA	H3663	WB	1:1000	Sigma	–
Ki67	D2H10	IHC	1:400	Cell Signaling	H
p-Chk2 (Thr68)	C13C1	WB	1:1000	Cell Signaling	H
RNF43	HPA008079	IHC	1:1000	Invitrogen (ATLAS)	H
RNF43	8D6	IF	1:150	–	H
K48-linked Ubiquitin	D9D5	WB	1:1000	Cell Signaling	H
K63-linked Ubiquitin	D7A11	WB	1:1000	Cell Signaling	H
γH2Ax	ab81299	WB, IHC, IF	1:10000 (WB) 1:5000 (IHC) 1:300 (IF)	Abcam	H, M
γH2Ax	5438	IP	1:50	Cell Signaling	H, M

GAPDH, glyceraldehyde-3-phosphate dehydrogenase; H, human; IF, immunofluorescence; IHC, immunohistochemistry; IP, immunoprecipitation; M, mouse; WB, Western blot.

After 1 week, organoids were incubated with 5-fluorouracil (2 μg/mL) or cisplatin (10 μg/mL) for 4 (murine) or 5 (human) days. Viability was analyzed using Cell Titer Glo 3D (Promega). Luminescence was measured using a SpectraMax plate reader (Molecular Devices, San José, CA). Viability was normalized to untreated controls. For human organoids, an organoid viability normalized to control greater than 95% was defined as a nonresponder, while organoids with a viability of less than 95% were defined as responders.

Animal Experiments

Friend Virus B NIH Jackson (FVBN) WT and *Rnf43*$^{\Delta Ex8}$ mice[13] were used for in vivo experiments. *Rnf43*$^{\Delta Ex8}$ mice were generated by introducing a 57-bp deletion in exon 8 of the genomic sequence of *Rnf43* using CRISPR/Cas9 technology. This deletion led to a systemic loss of the functional RING domain of Rnf43. Mice were co-housed under specific pathogen-free conditions in individually ventilated cages (Tecniplast, Hohenpeißenberg, Germany) containing enrichment material. Mice were fed a rodent diet (Envigo, Indianapolis, IN) ad libitum.

Eight- to 10-week-old male and female FVBN WT or *Rnf43*$^{\Delta Ex8}$ mice were infected twice with 2*10^8 *H pylori* PMSS1 diluted in 200 μL Brain heart infusion (BHI) 20% fetal calf serum by oral gavage. Mice were killed after 3 months.

Xenograft tumors were established as previously described.[13] Tumor volume was measured with a caliper and calculated as follows: volume = length*width*height/2. When tumors reached a volume of 40–70 mm^3, mice were injected with 20 mg/kg 5-fluorouracil or 10 mg/kg cisplatin twice a week. When tumors reached a size of 500 mm^3, mice were killed and tumors were resected.

Immunohistochemistry

Mouse gastric samples were fixed in 4% formaldehyde and embedded in paraffin. Heat-induced antigen retrieval was performed using 10 mmol/L sodium citrate (pH 6). Primary antibodies were applied overnight (Table 5), and bound secondary antibodies were detected with di-aminobenzidine. Slides were scanned and analyzed using an Olympus Virtual Slide Imaging System.

Sequencing

H&E-stained sections of gastric biopsy specimens were used to select the lesion to be analyzed. Sections (10-μm) were used to extract DNA with a GeneRead DNA FFPE Kit (Qiagen, Hilden, Germany). DNA concentrations were determined by a QuiBit 2.0 fluorometer (ThermoFisher, Waltham, MA) and the amplifiable genomic DNA was quantified using TaqMan RNase P detection kit (ThermoFisher). Barcoded libraries were generated using the Ion Xpress Barcode Adapters (ThermoFisher). Samples were purified using the Agencourt AMPure XP kit (Beckman Coulter) and quantified with the Ion Library TaqMan quantitation kit (Thermo-Fisher). Libraries were loaded on the Ion 530 chip kit (ThermoFisher) and sequenced using an Ion S5XL sequencer (ThermoFisher).

Statistics

Data were first tested for normality using the Shapiro–Wilk test. Normally distributed data then were analyzed by the Student t test. The Mann–Whitney U test or the Kruskal–Wallis test for multiple comparisons was used to compare not normally distributed data. Results of at least 3 independent experiments were analyzed. Statistical significance was defined when $P < .05$.

Study Approval

Experiments with human gastric organoids were approved by the Ethics Committee of Klinikum Rechts der Isar (116/17 S).

All animal experiments were conducted in compliance with European guidelines for the care and use of laboratory animals and were approved by the Regierung von Oberbayern (AZ 55.2-1-55-2532-239-15 and AZ 55.2-1-54-2532-196-2016).

Formalin-fixed, paraffin-embedded human gastric samples (Table 1) were obtained from the tissue bank of the Institut für Pathologie at Klinikum Bayreuth (Germany) after approval of the local ethics committee (Project number 243_19Bc).

All authors had access to the study data and reviewed and approved the final manuscript.

References

1. Lauren P. Histogenesis of intestinal and diffuse types of gastric carcinoma. Scand J Gastroenterol Suppl 1991;180:160–164.
2. Correa P. Human gastric carcinogenesis: a multistep and multifactorial process–First American Cancer Society Award Lecture on Cancer Epidemiology and Prevention. Cancer Res 1992;52:6735–6740.
3. Cancer Genome Atlas Research Network. Comprehensive molecular characterization of gastric adeno-carcinoma. Nature 2014;513:202–209.
4. Orditura M, Galizia G, Sforza V, Gambardella V, Fabozzi A, Laterza MM, Andreozzi F, Ventriglia J, Savastano B, Mabilia A, Lieto E, Ciardiello F, De Vita F. Treatment of gastric cancer. World J Gastroenterol 2014;20:1635–1649.
5. Aichler M, Luber B, Lordick F, Walch A. Proteomic and metabolic prediction of response to therapy in gastric cancer. World J Gastroenterol 2014;20:13648–13657.
6. Kim ST, Cristescu R, Bass AJ, Kim KM, Odegaard JI, Kim K, Liu XQ, Sher X, Jung H, Lee M, Lee S, Park SH, Park JO, Park YS, Lim HY, Lee H, Choi M, Talasaz A, Kang PS, Cheng J, Loboda A, Lee J, Kang WK. Comprehensive molecular characterization of clinical responses to PD-1 inhibition in metastatic gastric cancer. Nat Med 2018;24:1449–1458.

7. Lianos GD, Glantzounis GK, Bali CD, Katsios C, Roukos DH. Identification of novel genes by whole-exome sequencing can improve gastric cancer precision oncology. Future Oncol 2017;13:883–892.

8. Wang K, Yuen ST, Xu J, Lee SP, Yan HH, Shi ST, Siu HC, Deng S, Chu KM, Law S, Chan KH, Chan AS, Tsui WY, Ho SL, Chan AK, Man JL, Foglizzo V, Ng MK, Chan AS, Ching YP, Cheng GH, Xie T, Fernandez J, Li VS, Clevers H, Rejto PA, Mao M, Leung SY. Whole-genome sequencing and comprehensive molecular profiling identify new driver mutations in gastric cancer. Nat Genet 2014;46:573–582.

9. Maruvka YE, Mouw KW, Karlic R, Parasuraman P, Kamburov A, Polak P, Haradhvala NJ, Hess JM, Rheinbay E, Brody Y, Koren A, Braunstein LZ, D'Andrea A, Lawrence MS, Bass A, Bernards A, Michor F, Getz G. Analysis of somatic microsatellite indels identifies driver events in human tumors. Nat Biotechnol 2017;35:951–959.

10. Cho J, Ahn S, Son DS, Kim NK, Lee KW, Kim S, Lee J, Park SH, Park JO, Kang WK, An JY, Choi MG, Lee JH, Sohn TS, Bae JM, Kim S, Kim KM. Bridging genomics and phenomics of gastric carcinoma. Int J Cancer 2019;145:2407–2417.

11. Cho J, Chang YH, Heo YJ, Kim S, Kim NK, Park JO, Kang WK, Lee J, Kim KM. Four distinct immune microenvironment subtypes in gastric adenocarcinoma with special reference to microsatellite instability. ESMO Open 2018;3:e000326.

12. Jung SH, Kim SY, An CH, Lee SH, Jung ES, Park HC, Kim MS, Chung YJ, Lee SH. Clonal structures of regionally synchronous gastric adenomas and carcinomas. Clin Cancer Res 2018;24:4715–4725.

13. Neumeyer V, Grandl M, Dietl A, Brutau-Abia A, Allgauer M, Kalali B, Zhang Y, Pan KF, Steiger K, Vieth M, Anton M, Mejias-Luque R, Gerhard M. Loss of endogenous RNF43 function enhances proliferation and tumour growth of intestinal and gastric cells. Carcinogenesis 2019;40:551–559.

14. Koo BK, Spit M, Jordens I, Low TY, Stange DE, van de Wetering M, van Es JH, Mohammed S, Heck AJ, Maurice MM, Clevers H. Tumour suppressor RNF43 is a stem-cell E3 ligase that induces endocytosis of Wnt receptors. Nature 2012;488:665–669.

15. Loregger A, Grandl M, Mejias-Luque R, Allgauer M, Degenhart K, Haselmann V, Oikonomou C, Hatzis P, Janssen KP, Nitsche U, Gradl D, van den Broek O, Destree O, Ulm K, Neumaier M, Kalali B, Jung A, Varela I, Schmid RM, Rad R, Busch DH, Gerhard M. The E3 ligase RNF43 inhibits Wnt signaling downstream of mutated beta-catenin by sequestering TCF4 to the nuclear membrane. Sci Signal 2015;8:ra90.

16. Bohgaki M, Bohgaki T, El Ghamrasni S, Srikumar T, Maire G, Panier S, Fradet-Turcotte A, Stewart GS, Raught B, Hakem A, Hakem R. RNF168 ubiquitylates 53BP1 and controls its response to DNA double-strand breaks. Proc Natl Acad Sci U S A 2013; 110:20982–20987.

17. Doil C, Mailand N, Bekker-Jensen S, Menard P, Larsen DH, Pepperkok R, Ellenberg J, Panier S, Durocher D, Bartek J, Lukas J, Lukas C. RNF168 binds and amplifies ubiquitin conjugates on damaged chromosomes to allow accumulation of repair proteins. Cell 2009;136:435–446.

18. Mailand N, Bekker-Jensen S, Faustrup H, Melander F, Bartek J, Lukas C, Lukas J. RNF8 ubiquitylates histones at DNA double-strand breaks and promotes assembly of repair proteins. Cell 2007;131:887–900.

19. Pan MR, Peng G, Hung WC, Lin SY. Mono-ubiquitination of H2AX protein regulates DNA damage response signaling. J Biol Chem 2011; 286:28599–28607.

20. Smith J, Tho LM, Xu N, Gillespie DA. The ATM-Chk2 and ATR-Chk1 pathways in DNA damage signaling and cancer. Adv Cancer Res 2010;108:73–112.

21. Menoyo A, Alazzouzi H, Espin E, Armengol M, Yamamoto H, Schwartz S Jr. Somatic mutations in the DNA damage-response genes ATR and CHK1 in sporadic stomach tumors with microsatellite instability. Cancer Res 2001;61:7727–7730.

22. Kim JW, Im SA, Kim MA, Cho HJ, Lee DW, Lee KH, Kim TY, Han SW, Oh DY, Lee HJ, Kim TY, Yang HK, Kim WH, Bang YJ. Ataxia-telangiectasia-mutated protein expression with microsatellite instability in gastric cancer as prognostic marker. Int J Cancer 2014;134:72–80.

23. Touati E, Michel V, Thiberge JM, Wuscher N, Huerre M, Labigne A. Chronic Helicobacter pylori infections induce gastric mutations in mice. Gastroenterology 2003;124:1408–1419.

24. Butcher LD, den Hartog G, Ernst PB, Crowe SE. Oxidative stress resulting from Helicobacter pylori infection contributes to gastric carcinogenesis. Cell Mol Gastroenterol Hepatol 2017;3:316–322.

25. Toller IM, Neelsen KJ, Steger M, Hartung ML, Hottiger MO, Stucki M, Kalali B, Gerhard M, Sartori AA, Lopes M, Muller A. Carcinogenic bacterial pathogen Helicobacter pylori triggers DNA double-strand breaks and a DNA damage response in its host cells. Proc Natl Acad Sci U S A 2011;108:14944–14949.

26. Hartung ML, Gruber DC, Koch KN, Gruter L, Rehrauer H, Tegtmeyer N, Backert S, Muller AH. pylori-induced DNA strand breaks are introduced by nucleotide excision repair endonucleases and promote NF-kappaB target gene expression. Cell Rep 2015;13:70–79.

27. Santos JC, Gamboloni RZ, Roque AT, Oeck S, Ribeiro ML. Epigenetic mechanisms of ATM activation after Helicobacter pylori infection. Am J Pathol 2018; 188:329–335.

28. Smyth EC, Verheij M, Allum W, Cunningham D, Cervantes A, Arnold D; ESMO Guidelines Committee. Gastric cancer: ESMO Clinical Practice Guidelines for diagnosis, treatment and follow-up. Ann Oncol 2016; 27(Suppl 5):v38–v49.

29. Wen D, Wang G, Huang Z, Cui X, Song J, Zhu Z, Cui L. Reduced frequency and prognostic significance of ring finger protein 43 nucleotide polymorphisms in a Chinese colorectal cancer cohort. DNA Cell Biol 2019; 38:541–548.

30. Min BH, Hwang J, Kim NK, Park G, Kang SY, Ahn S, Ahn S, Ha SY, Lee YK, Kushima R, Van Vrancken M, Kim MJ, Park C, Park HY, Chae J, Jang SS, Kim SJ, Kim YH, Kim JI, Kim KM. Dysregulated Wnt signalling and recurrent mutations of the tumour suppressor RNF43 in early gastric carcinogenesis. J Pathol 2016; 240:304–314.

31. Wang H, Wang L, Erdjument-Bromage H, Vidal M, Tempst P, Jones RS, Zhang Y. Role of histone H2A ubiquitination in Polycomb silencing. Nature 2004; 431:873–878.

32. Wang B, Elledge SJ. Ubc13/Rnf8 ubiquitin ligases control foci formation of the Rap80/Abraxas/Brca1/Brcc36 complex in response to DNA damage. Proc Natl Acad Sci U S A 2007; 104:20759–20763.

33. Mattiroli F, Vissers JH, van Dijk WJ, Ikpa P, Citterio E, Vermeulen W, Marteijn JA, Sixma TK. RNF168 ubiquitinates K13-15 on H2A/H2AX to drive DNA damage signaling. Cell 2012;150:1182–1195.

34. Wu CY, Kang HY, Yang WL, Wu J, Jeong YS, Wang J, Chan CH, Lee SW, Zhang X, Lamothe B, Campos AD, Darnay BG, Lin HK. Critical role of monoubiquitination of histone H2AX protein in histone H2AX phosphorylation and DNA damage response. J Biol Chem 2011; 286:30806–30815.

35. Kim IH. Current status of adjuvant chemotherapy for gastric cancer. World J Gastrointest Oncol 2019; 11:679–685.

36. Gao Y, Cai A, Xi H, Li J, Xu W, Zhang Y, Zhang K, Cui J, Wu X, Wei B, Chen L. Ring finger protein 43 associates with gastric cancer progression and attenuates the stemness of gastric cancer stem-like cells via the Wnt-beta/catenin signaling pathway. Stem Cell Res Ther 2017;8:98.

37. Yamamoto H, Imai K. Microsatellite instability: an update. Arch Toxicol 2015;89:899–921.

38. Jackson SP, Bartek J. The DNA-damage response in human biology and disease. Nature 2009; 461:1071–1078.

39. Tu J, Park S, Yu W, Zhang S, Wu L, Carmon K, Liu QJ. The most common RNF43 mutant G659Vfs*41 is fully functional in inhibiting Wnt signaling and unlikely to play a role in tumorigenesis. Sci Rep 2019; 9:18557.

40. Gala MK, Mizukami Y, Le LP, Moriichi K, Austin T, Yamamoto M, Lauwers GY, Bardeesy N, Chung DC. Germline mutations in oncogene-induced senescence pathways are associated with multiple sessile serrated adenomas. Gastroenterology 2014;146:520–529.

41. Arnold IC, Lee JY, Amieva MR, Roers A, Flavell RA, Sparwasser T, Muller A. Tolerance rather than immunity protects from Helicobacter pylori-induced gastric preneoplasia. Gastroenterology 2011;140:199–209.

42. Bartfeld S, Clevers H. Organoids as model for infectious diseases: culture of human and murine stomach organoids and microinjection of Helicobacter pylori. J Vis Exp 2015;105:53359.

Correspondence
Address correspondence to: Raquel Mejías-Luque, PD, PhD, Trogerstrasse 30, Munich 81675, Germany. e-mail: raquel.mejias-luque@tum.de; fax: (49) 089-4140-4139.